November 26, 2021

Grand Mesa, Uncompahgre, and Gunnison National Forests
Attn: Plan Revision Team
2250 Highway 50
Delta, CO 81416
Submitted via the Online Feedback Tool

Re: Comments on the Draft Revised Land Management Plan and Draft Environmental Impact Statement for the Grand Mesa, Uncompahgre, and Gunnison National Forest

Dear GMUG Planning Team,

Thank you for considering the attached maps to inform the development of the GMUG revised plan. These maps are an aspect of the High Country Conservation Advocates (HCCA) et al comments submitted on November 24, 2021. In our comments, we addressed climate change in several places, including in relations to biodiversity, connectivity, and refugia. The maps below support these points. The maps were created by Alison Gallensky, Principal Conservation Geographer at Rocky Mountain Wild, who can be reached at alison@rockymountainwild.org. We welcome you to contact Matt Reed of HCCA at 970.349.7104 or matt@hccacb.org Lauren McCain of Defenders of Wildlife at 720.943.0453 or lmccain@defenders.org with any questions.

Sincerely,

Matt Reed
Public Lands Director
High Country Conservation Advocates
PO Box 1066
Crested Butte, CO 81224
970.349.7104
matt@hccacb.org

Lauren McCain
Senior Federal Lands Policy Analyst
Defenders of Wildlife
600 17th Street, Suite 450N
Denver, CO 80202
720.943.0453
lmccain@defenders.org

Forest Biomass Map

The Forest Biomass map below shows data from the USDA Forest Service of areas across the GMUG region with moderate to high concentrations of biomass, a measure of carbon storage. Biomass data downloaded to create this map are from https://data.fs.usda.gov/geodata/rastergateway/biomass/ on 11/22/2021. These data are also described in this article (attached): J.A. Blackard, M.V. Finco, E.H. Helmer, G.R. Holden, M.L. Hoppus, D.M. Jacobs, A.J. Lister, G.G. Moisen, M.D. Nelson, R. Riemann, B. Ruefenacht, D. Salajanu, D.L Weyermann, K.C. Winterberger, T.J. Brandeis, R.L. Czaplewski, R.E. McRoberts, P.L. Patterson, R.P. Tymcio, Mapping U.S. forest biomass using nationwide forest inventory data and moderate resolution information, *Remote Sensing of Environment*, Volume 112, Issue 4, 2008, Pages 1658-1677, ISSN 0034-4257, https://doi.org/10.1016/j.rse.2007.08.021.

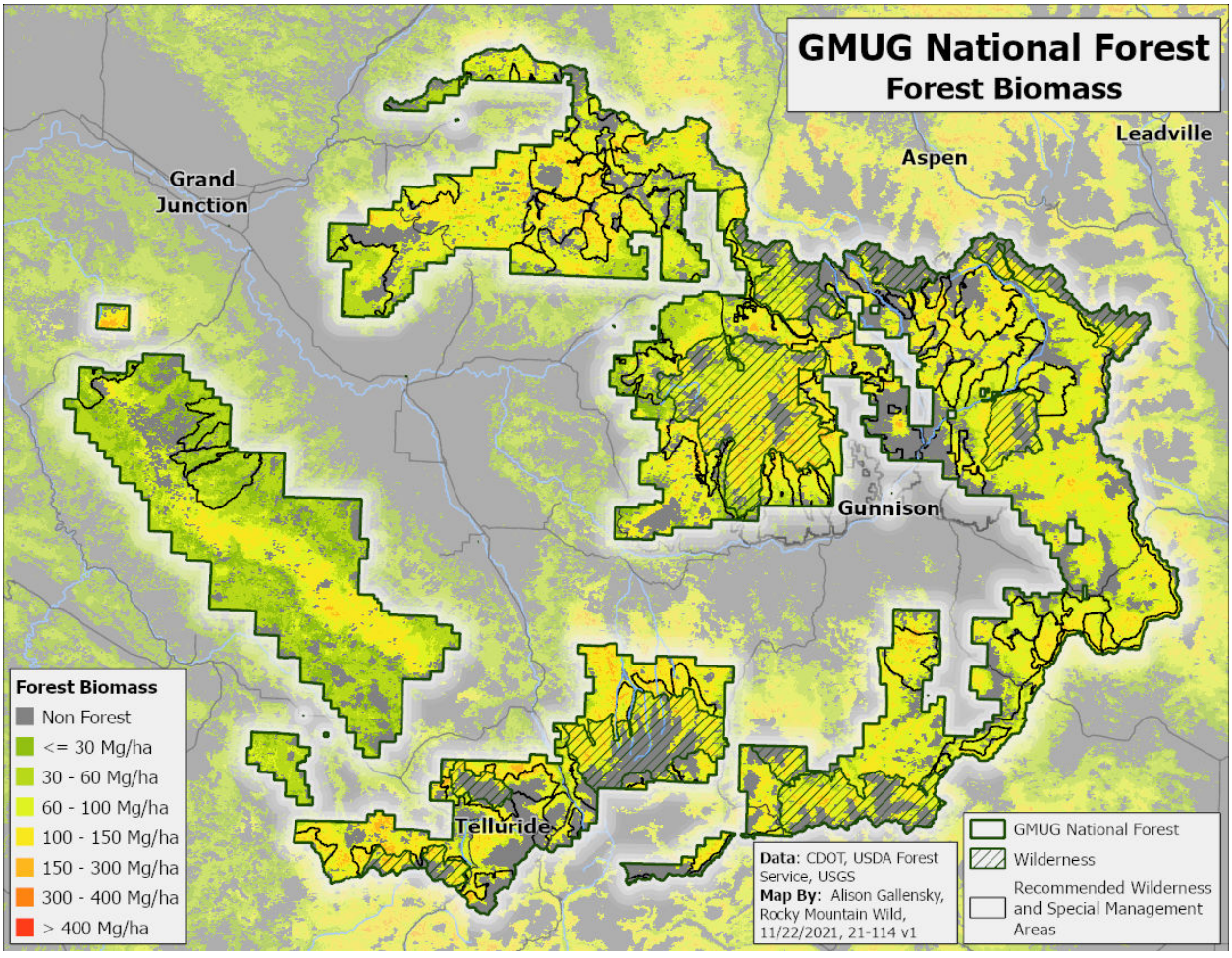

Climate Refugia and Corridors Map

The Climate Refugia and Corridors map below overlays areas of climate refugia and corridors that have been identified at the Center for Conservation Innovation of Defenders or Wildlife by a suite of different models. This modeling is described in the article: Dreiss, L. M., Lacey, L. M., Weber, T. C., Delach, A., Niederman, T. E., & Malcom, J. W. (2021). Targeting current species ranges and carbon stocks fails to conserve biodiversity in a changing climate: opportunities to support climate adaptation under 30x30. *bioRxiv*. *In press*. Attached and found here: https://www.biorxiv.org/content/10.1101/2021.08.31.458416v1.full.pdf

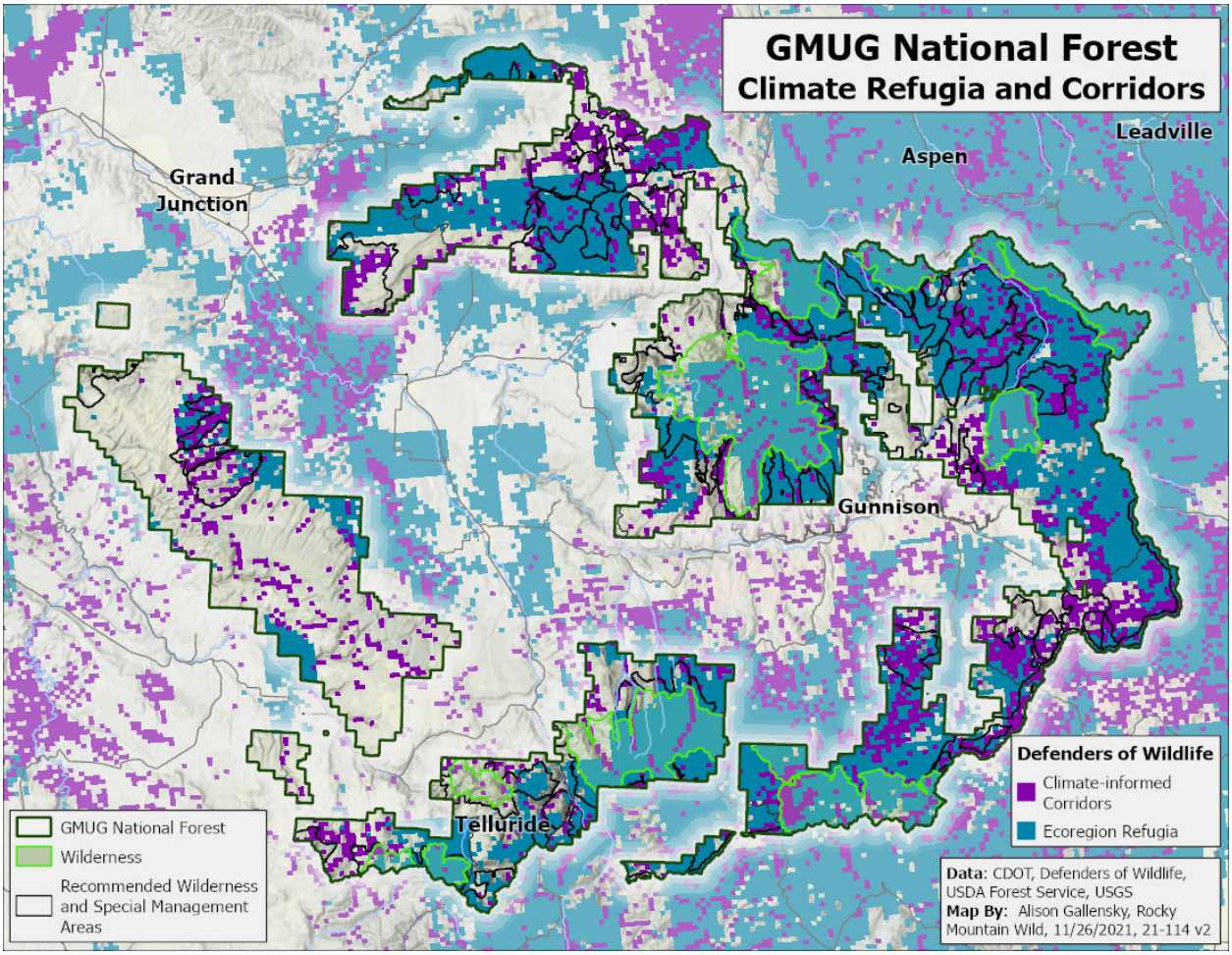

Resilient and Connected Network Map

The Resilient and Connected Network map below shows a proposed conservation network, identified by The Nature Conservancy, of representative climate-resilient sites designed to sustain biodiversity and ecological functions into the future under a changing climate. The Resilient and Connected Network data shown on this map were downloaded from: http://www.conservationgateway.org/ConservationPractices/ClimateChange/Pages/RCN-Downloads.aspx on 11/26/2021. The modeling techniques used to create this Network are described in a number of reports by The Nature Conservancy, including: Anderson, M.G., M. M. Clark, A. Olivero, and J. Prince. 2019. Resilient Sites and Connected Landscapes for Terrestrial Conservation in the Rocky Mountain and Southwest Desert Region. The Nature Conservancy, Eastern Conservation Science. https://tnc.app.box.com/s/cqz4dp69e34mptqml7anfr5ezy94hcyu

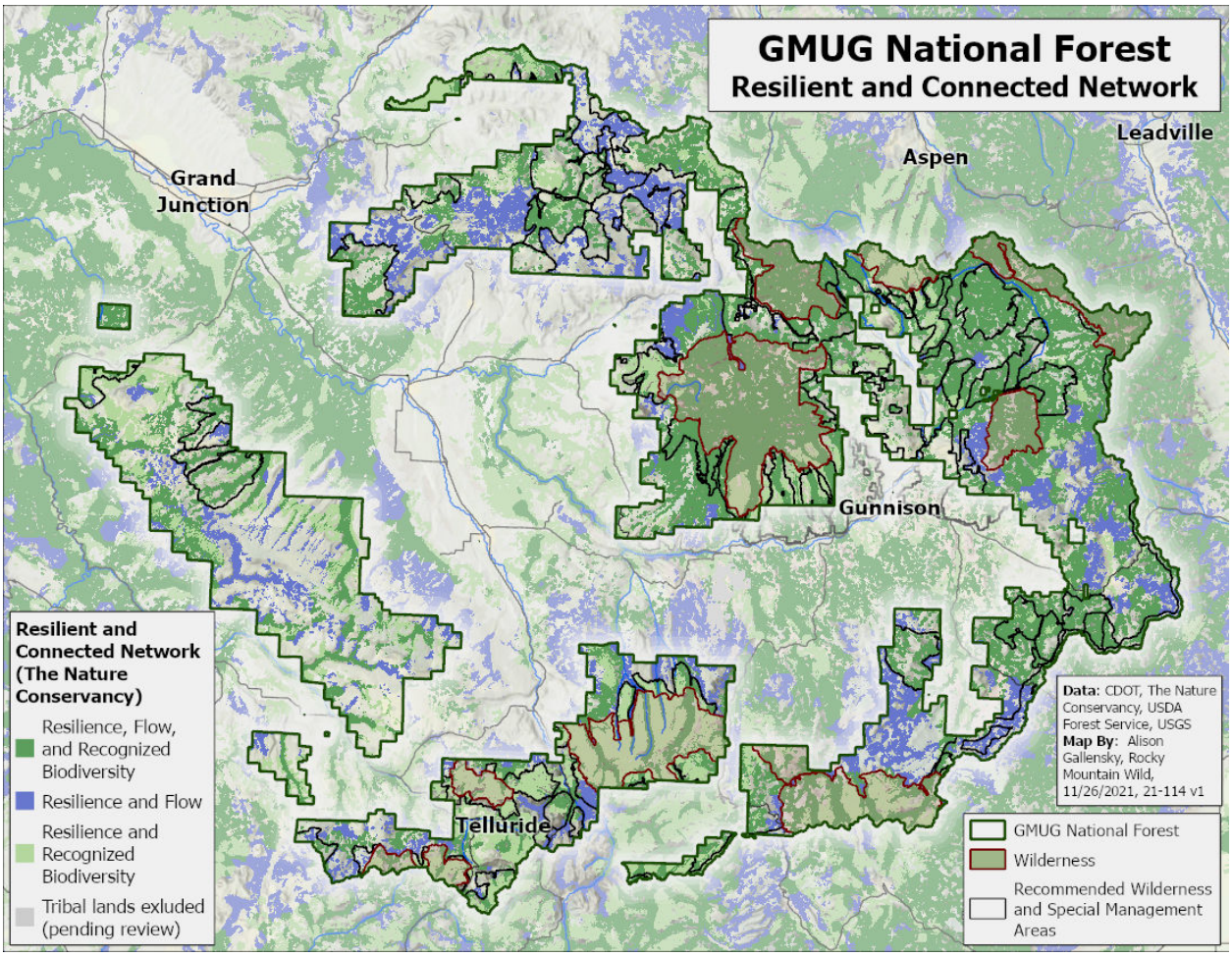

Available online at www.sciencedirect.com
ScienceDirect
Remote Sensing of Environment 112 (2008) 1658–1677
Remote Sensing of Environment
www.elsevier.com/locate/rse

Mapping U.S. forest biomass using nationwide forest inventory data and moderate resolution information

J.A. Blackard [a], M.V. Finco [b], E.H. Helmer [c], G.R. Holden [d], M.L. Hoppus [e], D.M. Jacobs [f], A.J. Lister [e], G.G. Moisen [a,*], M.D. Nelson [d], R. Riemann [e], B. Ruefenacht [b], D. Salajanu [f], D.L Weyermann [g], K.C. Winterberger [h], T.J. Brandeis [f], R.L. Czaplewski [i], R.E. McRoberts [d], P.L. Patterson [a], R.P. Tymcio [a]

[a] *Rocky Mtn. Research Station, 507 25th Street, Ogden, UT 84401, United States*
[b] *Remote Sensing Applications Center, 2200 W 2300 S, Salt Lake City, UT 84119, United States*
[c] *International Institute of Tropical Forestry, Jardín Botánico Sur, 1201 Calle Ceiba, Rio Piedras, 00926, Puerto Rico*
[d] *North Central Research Station, 1992 Folwell Ave, St. Paul, MN 55108, United States*
[e] *Northeastern Research Station, 11 Campus Blvd, Newtown Square, PA 19073, United States*
[f] *Southern Research Station, 4700 Old Kingston Pike, Knoxville, TN 37919, United States*
[g] *Pacific Northwest Research Station, 1221 SW Yamhill, Portland, OR 97205, United States*
[h] *Pacific Northwest Research Station, 3301 C St, Anchorage, AK 99503, United States*
[i] *Rocky Mtn Research Station, 240 W Prospect Rd, Fort Collins, CO 80526, United States*

Received 20 December 2005; received in revised form 24 August 2007; accepted 24 August 2007

Abstract

A spatially explicit dataset of aboveground live forest biomass was made from ground measured inventory plots for the conterminous U.S., Alaska and Puerto Rico. The plot data are from the USDA Forest Service Forest Inventory and Analysis (FIA) program. To scale these plot data to maps, we developed models relating field-measured response variables to plot attributes serving as the predictor variables. The plot attributes came from intersecting plot coordinates with geospatial datasets. Consequently, these models serve as mapping models. The geospatial predictor variables included Moderate Resolution Imaging Spectrometer (MODIS)-derived image composites and percent tree cover; land cover proportions and other data from the National Land Cover Dataset (NLCD); topographic variables; monthly and annual climate parameters; and other ancillary variables. We segmented the mapping models for the U.S. into 65 ecologically similar mapping zones, plus Alaska and Puerto Rico. First, we developed a forest mask by modeling the forest vs. nonforest assignment of field plots as functions of the predictor layers using classification trees in See5©. Secondly, forest biomass models were built within the predicted forest areas using tree-based algorithms in Cubist©. To validate the models, we compared field-measured with model-predicted forest/nonforest classification and biomass from an independent test set, randomly selected from available plot data for each mapping zone. The estimated proportion of correctly classified pixels for the forest mask ranged from 0.79 in Puerto Rico to 0.94 in Alaska. For biomass, model correlation coefficients ranged from a high of 0.73 in the Pacific Northwest, to a low of 0.31 in the Southern region. There was a tendency in all regions for these models to over-predict areas of small biomass and under-predict areas of large biomass, not capturing the full range in variability. Map-based estimates of forest area and forest biomass compared well with traditional plot-based estimates for individual states and for four scales of spatial aggregation. Variable importance analyses revealed that MODIS-derived information could contribute more predictive power than other classes of information when used in isolation. However, the true contribution of each variable is confounded by high correlations. Consequently, excluding any one class of variables resulted in only small effects on overall map accuracy. An estimate of total C pools in live forest biomass of U.S. forests, derived from the nationwide biomass map, also compared well with previously published estimates.

Keywords: Forest biomass; MODIS; Classification and regression trees; Forest probability; Carbon; FIA

* Corresponding author. USDA Forest Service, Rocky Mountain Research Station, 507 25th Street, Ogden, UT 84401, United States, Tel.: +1 801 625 5384; fax: +1 801 625 5723.
E-mail address: gmoisen@fs.fed.us (G.G. Moisen).

0034-4257/$ - see front matter © 2007 Elsevier Inc. All rights reserved.
doi:10.1016/j.rse.2007.08.021

1. Introduction

The Forest Inventory and Analysis (FIA) program of the USDA Forest Service collects data annually on the status and trends in forested ecosystems nationwide. These inventory data support estimates of forest population totals over large geographic areas, (Scott et al., 2005). Regional maps of forest characteristics would make these extensive forest resource data more accessible and useful to a larger and more diverse audience. Important applications of such maps include broad-scale mapping and assessment of wildlife habitat; documenting forest resources affected by fire, fragmentation, and urbanization; identifying land suitable for timber production; and locating areas at high risk for plant invasions, or insect or disease outbreaks. Thus, there is a need to produce and distribute geospatial data of forest attributes, complementing FIA inventory data.

Total aboveground live biomass is a forest characteristic of particular interest. Forest soils and woody biomass hold most of the carbon in Earth's terrestrial biomes (Houghton, 1999). Land-use change, mainly forest burning, harvest, or clearing for agriculture, may compose 15 to 40% of annual human-caused emissions of carbon to the atmosphere, and terrestrial ecosystems, mainly through forest growth and expansion, absorb nearly as much carbon annually. However, estimates of land-atmosphere carbon fluxes, and the net of expected future ones, have the largest uncertainties in the global atmospheric carbon budget, which adds to uncertainties about future levels and impacts of greenhouse gasses (GHGs) in the atmosphere (Houghton, 2003; Prentice et al., 2001).

Consequently, the levels, mechanisms and spatial distribution of forest land-atmosphere C fluxes are an important focus for reducing uncertainties in the global C budget (Fan et al., 1998; Holland et al., 1999; Pacala et al., 2001; Schimel et al., 2001). Ecosystem process models that are physiologically-based, and that use satellite image-derived indices of photosynthesis, have permitted unprecedented global assessments of ecosystem productivity and carbon sinks at a spatial resolution of 0.5° (Nemani et al., 2003; Potter et al., 2003). The mechanistic nature of these models identifies how observed patterns in ecosystem productivity may relate to climate and atmospheric changes (Nemani et al., 2003). However, validating atmospheric and ecosystem model estimates of net forest C fluxes, and quantifying the C fluxes associated with changes in land use, which dominate these fluxes over longer time periods, requires spatially extensive data on forest C pools and net fluxes. Maps of forest biomass permit spatially explicit estimates of forest carbon storage and net fluxes from land-use change.

Our objectives here are to 1) produce a spatially explicit dataset of aboveground live forest biomass from ground measured inventory plots, at a 250-m cell size, for the conterminous U.S., Alaska and Puerto Rico; 2) evaluate model performance and spatially depict uncertainty in the dataset; 3) explore the relative contribution of the many predictor layers to the biomass models; and 4) use the resulting dataset to estimate aboveground live forest biomass and implied carbon storage for this area. We also describe a national geospatial predictor database that supported the mapping and how we standardized national FIA data, developed predictive models, and assessed model error.

2. Methods

2.1. Data

2.1.1. Response variables

The US Forest Service FIA program inventories the Nation's forests via a network of ground-based inventory plots in which forest structure and tree species composition are measured to produce estimates of forest attributes like basal area by species, total volume, and total biomass. Plots are located with an intensity of about one plot per 2400 ha. Although the program historically collected data periodically (every 5 to 20 years) for each state in the country, it recently shifted to an annual rotating panel system. This new system samples 10 to 20% of each state's plot network annually (Bechtold & Patterson, 2005). This study used a mixture of annual and historic periodic data to ensure enough training plots in all parts of the country, with dates of collection ranging between 1990 and 2003. The advantages of modeling response variables collected from a probabilistic sample (such as FIA's plot network) over those collected from a purposive sample are explored in Edwards et al. (2006).

The FIA program observes, measures, and predicts many forest attributes on each plot (Miles et al., 2001). This nationwide biomass mapping effort modeled two of these plot-level response variables: a binary forest/nonforest classification and aboveground live forest biomass. According to FIA definitions, *forest land* is at least 0.405 ha in size, has a minimum continuous canopy width of 36.58 m with at least 10% stocking, and has an understory undisturbed by a nonforest land use like residences or agriculture. *Aboveground live biomass* includes biomass in live tree bole wood, stumps, branches and twigs for trees 2.54-cm diameter or larger and is derived from region- or species-specific allometric equations.

2.1.2. National geospatial predictor layers

A nationwide geospatial dataset of layers of predictor variables, also called the national geospatial predictor layer database, was assembled for use in the biomass models. The data layers included satellite imagery and predicted land-cover from Moderate Resolution Imaging Spectro-radiometer (MODIS) (Justice et al., 2002), Landsat Thematic Mapper image-derived National Land Cover Dataset (NLCD92, Vogelmann et al., 2001), raster climate data, and topographic variables. Datasets with native spatial resolutions other than 250 m were resampled with a nearest neighbor procedure if categorical, and a bilinear interpolation procedure if continuous. The 250-m spatial resolution of the predictor dataset has two origins. First, the coarser spatial scale of MODIS would be practical given the national extent of the project, and the MODIS sensor bands 1 and 2 are available at that spatial resolution. As a result, MODIS vegetation index data are available with 250-m pixel sizes. Secondly, we expected that coarser image data would have scaling advantages when working with passive optical imagery, as we discuss later.

Data from MODIS for the year 2001 included all land surface reflectance bands (Vermote & Vermueulen, 1999) (MOD 09v003) from three 8-day image composites at 500-m resolution (beginning Julian days 097, 225, 321), three 16-day vegetation index (VI) composites (Huete et al., 2002) (MOD 13v003) at 250-m resolution over the same three compositing periods, and percent tree cover (MOD 44) at 500-m resolution for 2001 (Hansen et al., 2003). The compositing periods represented early, peak, and leaf-off phenological conditions in the continental United States. For Puerto Rico, persistent cloudiness necessitated data from dry-season MODIS image compositing periods, including six periods from 2001–2003. The MOD 09 8-day image composites use a minimum-blue criterion to select for clearest conditions (Vermote & Vermueulen, 1999). The compositing algorithm for MOD 13 VI data first selects clear pixels over the compositing period with the MODIS cloud mask. A pixel-level fit to a bidirectional reflectance distribution function (BRDF) then estimates a near-nadir reflectance for each band for calculating VI values. If fewer than five pixels are clear over the compositing period, then the algorithm selects a clear pixel based on viewing angle. Otherwise, the algorithm selects the pixel with the maximum Normalized Difference Vegetation Index (NDVI) (Huete et al., 2002). We performed no additional image compositing or cloud filling for continental U.S. imagery. Some cloudy areas were masked from the Puerto Rico composites and filled with appropriate composite imagery from other dates.

Landsat image-based land cover for the conterminous U.S. (Vogelmann et al., 2001) and Puerto Rico (Helmer et al., 2002) provided data on proportional cover of forest, shrubland, wetland and urban/barren lands (Puerto Rico only). These 30-m components of the national geospatial predictor data used focal functions to summarize the land cover class proportions within a 9×9 moving window and subsequently resampled the data to 250-m with bilinear resampling. Climate data included 30-year (1961–1990) average monthly and annual precipitation and temperature measures, represented by spatial resolutions of about 4 km for the conterminous U.S. (Daly et al., 2000), 2 km for Alaska (Daly, 2002) and 420-m for Puerto Rico (Daly et al., 2003). The dataset also included elevation from 30-m digital elevation models (DEMs) (Gesch et al., 2002), and other topographic derivatives from those DEMs, including slope, dominant aspect, and an indicator of aspect variety. This indicator is calculated as the total number of unique aspect values (or the variety) within the nine by nine window surrounding each 30-m cell. The resulting dataset was resampled to a 250-m cell size. The same resampling method used for the 30-m Landsat products (described above) was used to summarize the elevation-based attributes at 250-m. A final topographic variable that several models used was a horizontal-distance-to-nearest-stream measure, which is the Euclidean distance from each pixel to its nearest above-ground water body, as the crow flies.

2.2. Modeling strategy

2.2.1. Process overview

We created a nationwide modeling dataset by intersecting plot locations with the geospatial predictor layers, and extracting all relevant data. Resulting values of predictor layers for each plot were then linked to the corresponding forest/nonforest and forest biomass response variables. We segmented this modeling dataset into 65 ecologically unique mapping/modeling zones (Fig. 1) (Homer & Gallant, 2001) which permitted separate models to target the conditions unique to each zone. However, we aggregated adjacent zones in sparsely forested regions, which had too few forested plots, to increase the number of observations in the models for those zones. Independent test sets were created by randomly selecting 10 to 15% of the plots by mapping zone, leading to proportional distribution by zone. These test sets were withheld to assess model performance, except in Puerto Rico where insufficient numbers of plots forced the use of 10-fold crossvalidation for evaluating biomass model performance. Using classification trees with boosting for each mapping zone, we first produced a 250-m resolution forest mask by modeling the binary variable of forest/nonforest as a function of all the variables contained in the national geospatial predictor layers. We then selected only those FIA plots that fell within the forested portion of the forest mask as training data for the biomass models. Regression tree algorithms were then used to model forest biomass (also at 250 m) as a function of those same predictor variables used in the forest/nonforest models for each mapping zone. Because of ecological differences between zones, the way in which the classification trees used and partitioned the predictor variables was very different by zone. Also, some regional variations in the methods themselves were used to improve the forest/nonforest and biomass models. Examples include inclusion of regional specific predictor layers and larger groupings of similar mapping zones. We then predicted forest biomass on a per-pixel basis by applying the models developed for each mapping zone to the corresponding predictor layers for that zone. Pixels with nonforest class label predictions were omitted from subsequent analyses, and labeled as having no forest biomass. Finally, using the classification confidence and absolute error information available from the models, two additional geospatial datasets were created to capture the per-pixel uncertainty associated with each estimate – resulting in a map of forest probability, and a map of biomass percent error (details in section on Uncertainty maps). The individual zone maps of forest/nonforest, forest probability, biomass, and percent error for biomass were mosaiced to form nationwide datasets. A state boundary geospatial layer identified coastal shorelines (nationalatlas.gov/statesm.html), and a national hydrography layer (nationalatlas.gov/hydrom.html) delineated interior water boundaries.

2.2.2. Classification and regression trees

Classification and regression tree modeling, or recursive partitioning regression (Breiman et al., 1984), is available in many software packages and is now common in remote sensing applications. To give a general overview of the methodology, trees subdivide the space spanned by the predictor variables into regions for which the values of the response variable are most similar, and then assign a unique prediction for each of these regions. The tree is called a classification tree if the response variable is discrete and a regression tree if the response variable is

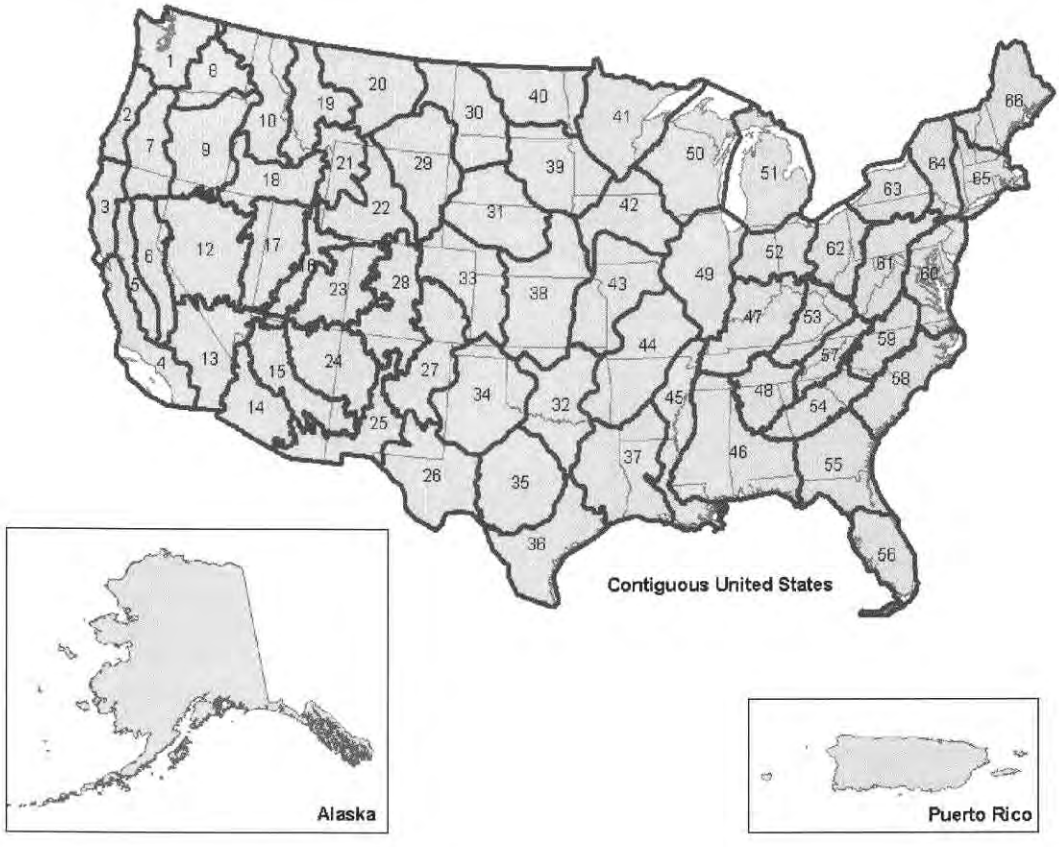

Fig. 1. Mapping/modeling zones (Homer & Gallant, 2001) segmented forest vs. nonforest and biomass classification and mapping models.

continuous. Tree-based methods have evolved to enhance their predictive capabilities. Two recent enhancements have had considerable success in mapping applications (Chan et al., 2001). One is known as bagging, or bootstrap aggregation (Bauer & Kohavi, 1998; Breiman, 1996). The other is called boosting (Freund & Schapire, 1996) with its variant Resampling and Combining (ARCing) (Breiman, 1998). These iterative themes each produce a committee of expert trees by resampling with replacement from the initial data set, then averaging the trees with a plurality voting scheme if the response is discrete, or simple averaging if the response is continuous. The difference between bagging and boosting is the type of data resampling. In bagging, all observations have equal probability of entering the next bootstrap sample. In boosting, problematic observations, those which are frequently misclassified, have a higher probability of selection. The performance of tree-based methods for modeling FIA response variables is compared to other modeling techniques in Moisen and Frescino (2002) and Moisen et al. (2006).

Specifically for this study, classification trees with boosting (5 or 10 trials) and pruning in See5 (www.rulequest.com, Quinlan, 1986, 1993) generated the forest mask based on a 0.5 threshold for distinguishing forest from nonforest. Cubist (www.rulequest.com) generated the mapping models of forest biomass within pixels predicted to be forested. Cubist is a proprietary variant on regression trees with piecewise nonoverlapping regression. Specific software options used for most mapping zones included the following: either 5 or 10 committee models; use of rules alone (no instances); minimum rule cover of 1% of cases; extrapolation up to 10%; and no maximum number of rules.

2.3. Model performance

Measures for assessing and depicting accuracies, errors, and uncertainties of the modeled spatial datasets were chosen by taking into consideration traditional methods of accuracy assessment, known characteristics of the datasets, and their anticipated uses.

2.3.1. Per-pixel measures

Accuracy and error measures for the forest mask included proportion of correctly classified units (PCC), Kappa (Cohen, 1960), as well as omission and commission errors for both the forest and nonforest classes. PCC is a statistic that can be deceptively high when the proportion of a class, in this case forest, is very low or very high. The Kappa statistic measures the proportion of correctly classified units after removing the probability of chance agreement. Errors of omission (1-producer's accuracy) result when a pixel is incorrectly classified into another category, thus being omitted from its correct class. Errors of commission (1-user's accuracy) result when a pixel is committed to an incorrect class. For the biomass map, the per-pixel accuracy measures that we calculated on the independent test sets included average absolute error,

relative error, and correlation. The average absolute error for a set of test cases is the average of the sizes of differences between the actual and predicted values for each case, expressed in metric tons per ha. The relative error is the ratio of the average absolute error to the average absolute error that would result by predicting the value of each case as the mean of the training set. Because it is normalized by the predicted value's unit of measure, the relative error term is useful for comparing the performance of different models. It also gives an indication of individual model performance above and beyond simply using the average value from the training data as its 'predicted' value. A relative error substantially less than one indicates that the model predictions are substantially better than simply using a prediction of the sample mean. The correlation coefficient is a standard measure of the linear relationship between observed and predicted values.

2.3.2. Uncertainty maps

One of the goals of this study was to provide spatially explicit depictions of the uncertainty in both the forest mask and forest biomass maps. Maps of uncertainty are derived from the modeling process itself and provide users (and developers) information on where the model was more and less confident of the estimate based on the training and predictor information available and the modeling technique used.

For the forest/nonforest map, a binary response variable, the need for a spatial depiction of uncertainty was satisfied with a forest probability dataset, depicting the probability that any individual pixel could be classified as forest. In many modeling applications for binary response variables, predictions are made on a continuum of 0 to 1, indicating probability of a pixel belonging to the class of interest. Because of the way in which See5 constructs predictions, a map of forest probability had to be back-engineered in the following way. First, the public C code distributed with See5 (http://rulequest.com/see5-public.zip) enabled us to produce a confidence value for each pixel prediction as a forest/nonforest classification confidence map. This software routine operates as follows: if a single classification tree is used and a case is classified by a single leaf of a decision tree, the confidence value assigned is the proportion of training cases at that terminal node that belongs to the predicted class. If more than one terminal node is involved, the confidence value assigned is a weighted sum of the individual nodes' confidences. If more than one tree is involved (eg. boosting), the value is a weighted sum of the individual trees' confidences. Second, a forest probability map was created by remapping confidence values from the public C code to a range of 0 to 0.5 for nonforest pixels and 0.5 to 1 for forest pixels, creating a new range from 0 to 1. Here, values near 0 indicate a more confident prediction for nonforest areas, values near 1.0 indicate a more confident prediction for forest areas, and values around 0.55 are the most uncertain.

For the map of aboveground forest biomass, spatial depictions of uncertainty took the form of biomass percent error maps. These were derived by first extracting the weighted average absolute error of all the rules that applied to each pixel, in which the average absolute error for each rule is from the training data. The biomass percent error map then resulted from dividing that weighted average absolute error by the predicted biomass value at that pixel. Such uncertainty maps provide information regarding both the location and magnitude of potential errors in the modeled estimates. They allow users to incorporate this information into all further modeling or analysis efforts using the estimated biomass and forestland maps/datasets (Fortin et al., 1999; Mowrer, 1994; Woodbury et al., 1998).

2.3.3. Agreement of spatial aggregations

FIA plot data is typically used to produce unbiased estimates of forest population totals using design-based inference (Cochran, 1977; Särdnal et al., 1992; Thompson, 1997) for areas of sufficient size. Often in practice, however, maps may be used to produce population estimates of these mapped variables by summing pixels over the geographic area of interest. This method relies on model-based inference (Valliant et al., 2001). To provide information on the comparative accuracy of these "map-based" estimates of area of forestland and total biomass, we compared them to "plot-based" estimates of total forest area and biomass by state for the US using FIA sample plots (Scott et al, 2005). Note that although FIA will use remote sensing information to stratify sample plots to improve precision in estimates of forest population totals, the plot-based estimates used here are solely based on field data. This comparison allows users of inventory data who are familiar with the traditional plot-based estimates to examine the location and magnitude of areas of over-and underestimation of map-based estimates.

Next, in order to examine the scales at which aggregated estimates of forest area or total forest biomass agree with plot-based estimates, we also made comparisons for hexagons at four different sizes: ~16,000, ~21,000, ~39,000, and ~65,000 ha. The hexagons were derived by tessellation from the Environmental Monitoring and Assessment Program hexagons (White et al., 1992) that are used as the basis for the FIA sampling design (Bechtold & Patterson, 2005). For both area of forestland and

Table 1
Per-pixel measures of performance for forest/nonforest maps based on independent test sets, reported by region

Region	PCC	Kappa	Omission forest	Commission forest	Omission nonforest	Commission nonforest	Test set sample size
Northeast	0.89	0.77	0.08	0.09	0.14	0.14	1181
Northcentral	0.93	0.80	0.15	0.15	0.05	0.05	5449
Interior West	0.91	0.76	0.17	0.18	0.07	0.06	7196
Pacific Northwest	0.85	0.61	0.05	0.15	0.39	0.15	2588
Southern	0.86	0.69	0.10	0.13	0.22	0.17	3138
Alaska	0.94	0.88	0.07	0.08	0.05	0.04	6553
Puerto Rico	0.79	0.57	0.07	0.28	0.36	0.10	28

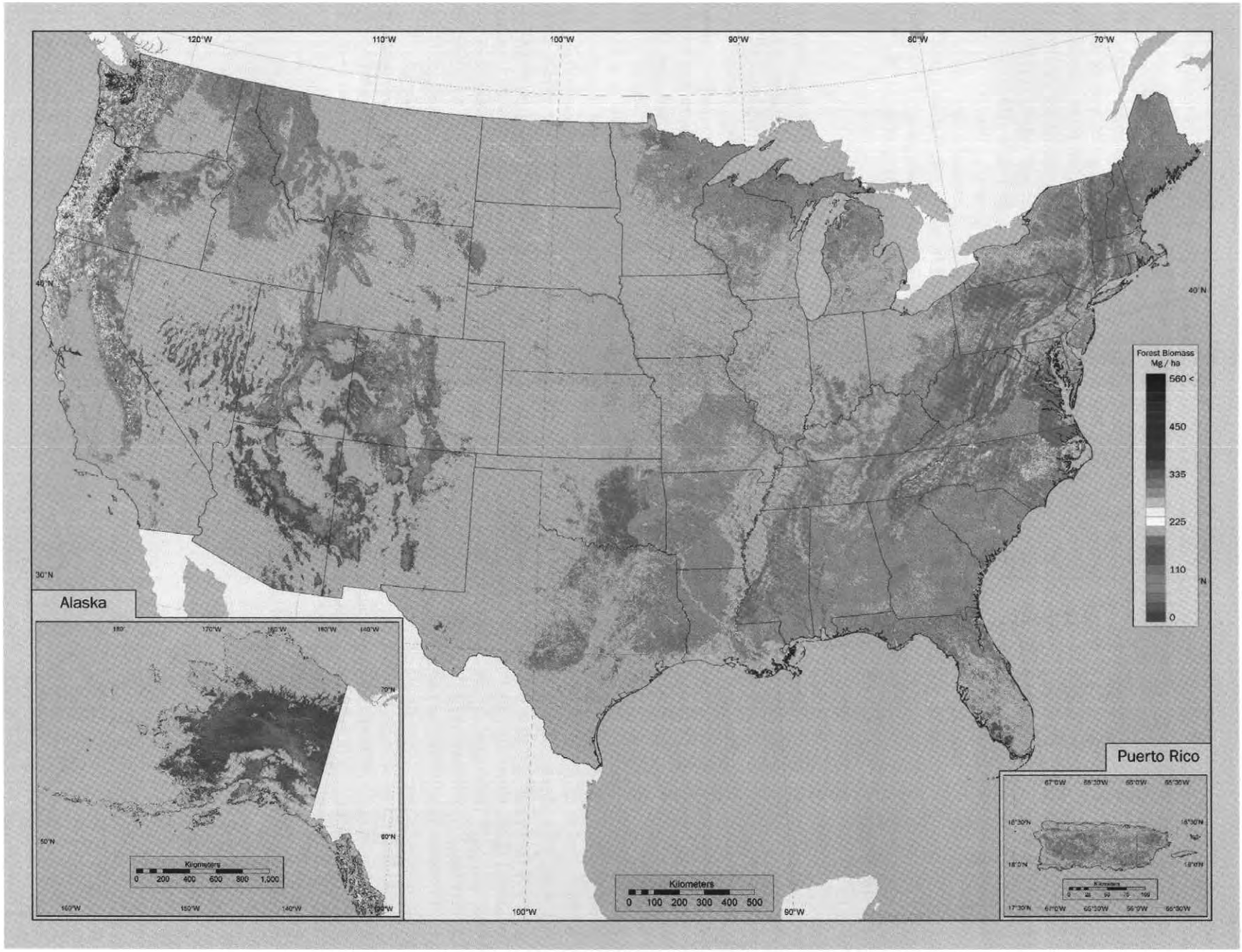

Fig. 2. A map of aboveground forest biomass (dry weight) in live trees, tumps, branches and twigs derived from modeling FIA plot biomass as a function of geospatial predictor variables.

Table 2
Per-pixel measures of performance for biomass maps based on independent test sets (except for Puerto Rico where 10-fold cross-validation was used), reported by region

Region	Average absolute error	Relative error	Correlation	Test set sample size
Northeast	60.1	0.89	0.39	1156
Northcentral	42.5	0.88	0.46	1134
Interior West	42.2	0.65	0.66	2023
Pacific Northwest	163.1	0.72	0.73	1591
Southern	60.2	0.92	0.31	1939
Alaska	91.5	0.59	0.69	430
Puerto Rico	65.0	0.51	0.92	*

*Based on a 10-fold cross validation.
Average absolute error is reported in metric tons per hectare.

aboveground forest biomass, agreement between the mean of pixel predictions for all pixels with centers in a hexagon to the mean of plot observations for all plots with centers in the hexagon was assessed as follows. For each hexagon, the mean pixel prediction, $\hat{\mu}_{\text{pixel}}$, for a hexagon was compared to the plot-based mean, $\hat{\mu}_{\text{plot}}$, using,

$$\tau = \frac{\hat{\mu}_{\text{pixel}} - \hat{\mu}_{\text{plot}}}{\text{SE}(\hat{\mu}_{\text{plot}})}$$

where $\text{SE}(\hat{\mu}_{\text{plot}})$ denotes the design-based standard error. Here, τ is not a formal statistic with an established distribution and probability levels. Rather it is constructed as a heuristic tool by with which to assess relative agreement between traditional plot-based estimates, and map-based estimates at varying scales of aggregation.

Arrays of hexagons of four sizes were considered: ~16,000 ha, ~21,000 ha, ~39,000 ha, and ~65,000 ha. Based on a sampling intensity of approximately one plot per 2400 ha, hexagons of ~16,000 ha would include 6–7 plots, about the smallest sample sizes that would yield reliable estimates of SE ($\hat{\mu}_{\text{plot}}$). Selection of the sizes of the larger hexagons was arbitrary, except for the ~65,000-ha EMAP hexagons, from which unique ID codes are attributed to FIA plots and which are used in several national assessments. For areas of the country in which a complete cycle of sampling has not been completed, some hexagons may include fewer than 6–7 plots. No comparisons of pixel-and plot-based means were calculated for hexagons with fewer than 5 plots. Tau-values exceeding 2 were interpreted as a conservative indication that model-based estimates disagreed with plot-based estimates within each hexagon.

2.3.4. Variable importance

A series of variable importance analyses were conducted to assess the relative contributions of the numerous predictor variables to the modeling process. First, the relative importance of the major groups of predictor variables were assessed in each region. This was measured by percent improvement, or decrease, in relative error when each major group was used alone as predictor sets in different models of biomass. Major groups were the "MODIS group" (including NDVI, Enhanced Vegetation Index [EVI], spectral bands, fire, and percent tree cover), the "Climate group" (including all precipitation variables), the "NLCD group" (including only NLCD-derived variables), and the "Topo group" (including topographic variables). Note that in Alaska and in Puerto Rico, no NLCD data were available, and surrogate variables labeled as the "Veg group" were used instead.

Next, the relative importance of sub-groups of the "MODIS group" were measured by percent improvement, or decrease, in relative error when each of these sub-groups was used exclusively in the models. These sub-groups were the "Bands sub-group" (including all MODIS bands, all dates), the "NDVI sub-group" (including al NDVI variables), "Treecov sub-group" (including percent tree cover), the "EVI sub-group" (including all EVI variables), and the "Fire sub-group" (including all fire-related variables).

Because the true contribution of each variable to the final biomass map is confounded by high correlation between variables, variable groups were excluded in turn from the original biomass model, and the effect on relative error examined. In addition, the potential effect on pixel aggregations were explored by examining changes in density functions of predicted values under the different models excluding variable groups in turn.

2.3.5. Estimates of C pools

Finally, estimates of C pools in live forest biomass of U.S. forests, derived from the map developed in this study, were compared with estimates from other national studies. Estimates of the mass of C for live trees, stumps, branches and twigs were obtained by summing one-half the predicted biomass for each pixel over the conterminous U.S., and Alaska. The one-half rule is based on Brown and Lugo (1992). Mass of C for roots was approximated as 20% of total predicted biomass (Cairns et al., 1997). Results were compared those obtained by Turner et al. (1995), Birdsey and Heath (1995), Potter (1999), and Dong et al. (2003).

3. Results

All maps produced in this study, including the forest/nonforest mask, forest probability, forest biomass, and biomass percent error, are available for download via http://svinetfc4.fs.fed.us/rastergateway/biomass/.

3.1. Per pixel measures

As illustrated in Table 1, the forest mask was reasonably accurate in all regions, with regional PCCs ranging from 0.79 in Puerto Rico to 0.94 in Alaska, and regional Kappa values ranged from 0.57 in Puerto Rico to 0.88 in Alaska, reflecting fair to excellent class agreement. Errors of omission for forest were generally low, ranging from 0.05 in the heavily forested Pacific Northwest to 0.17 in the more nonforested Interior West, while errors of commission for forest ranged from 0.08 in Alaska to 0.28 in Puerto Rico. Errors of omission for nonforest ranged from 0.05 in the Northcentral region and

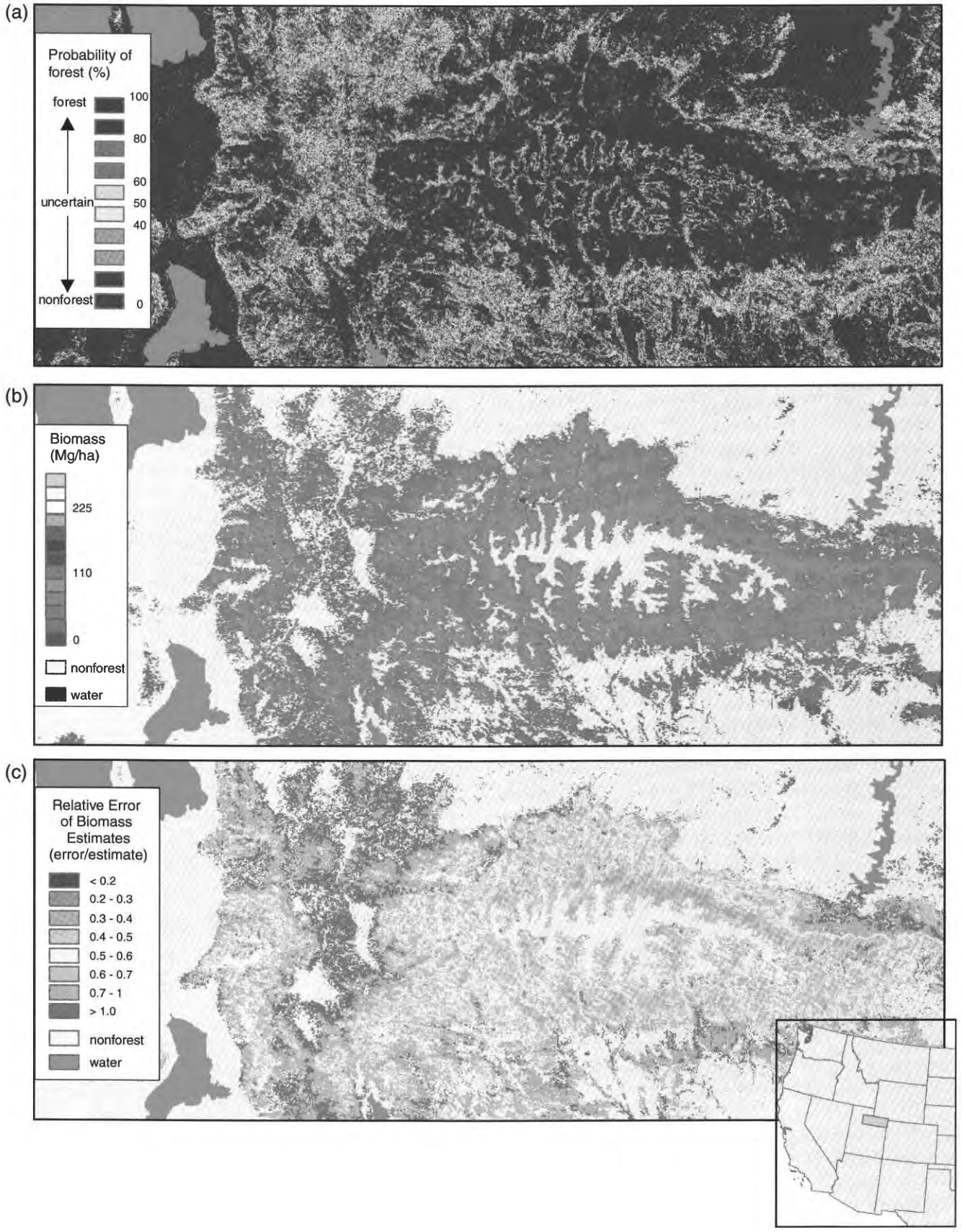

Fig. 3. Probability of forest, biomass, and percent error in biomass mapped over Uinta Mountains in Utah, (a, b, and c respectively). Probability of forest, biomass, and percent error in biomass mapped for the Greater Mohawk Valley Region, New York (d, e, and f respectively).

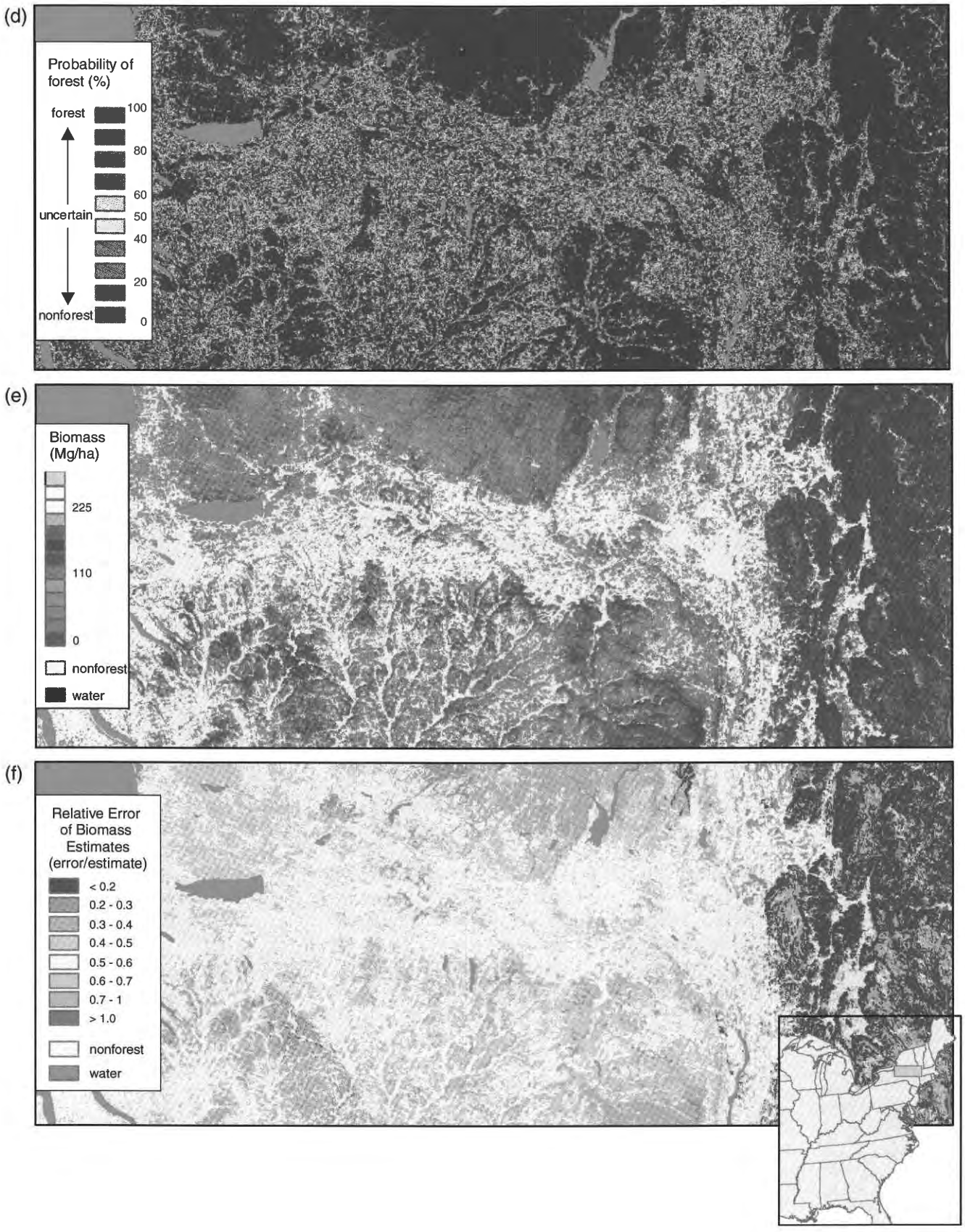

Fig. 3 (*continued*).

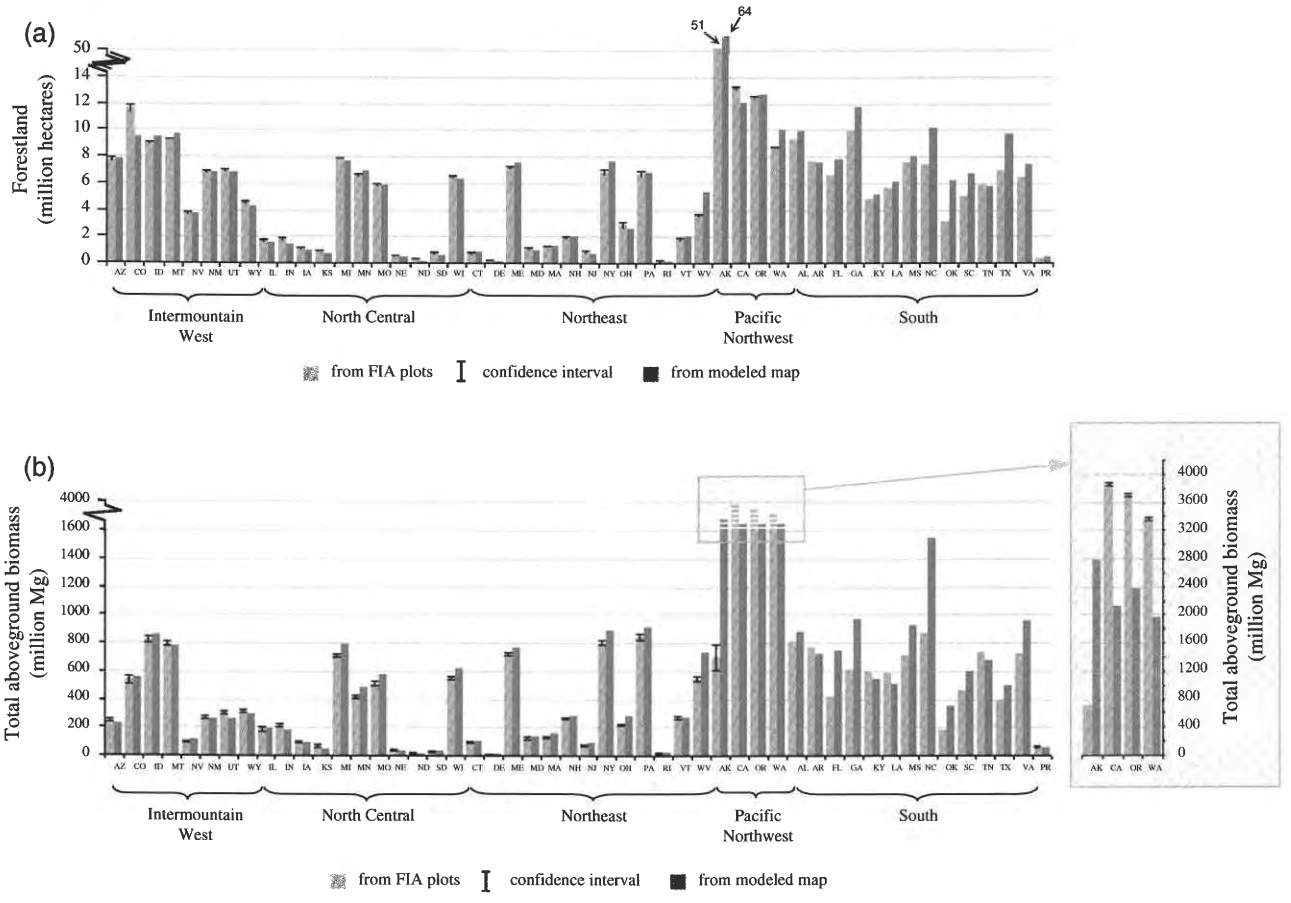

Fig. 4. Plot-based and map-based estimates of (a) forestland and (b) total forest biomass (dry weight), by state. States are grouped by USFS Forest Inventory and Analysis Region. A separate Y axis is provide for the Pacific Northwest states because of the substantially different scales involved.

Alaska to 0.39 in the Pacific Northwest, while errors of commission for nonforest ranged from 0.04 in Alaska to 0.17 in the Southern region. Per-pixel measures of performance for the forest/nonforest maps are given for individual and aggregated zones in Appendix A.

The forest biomass map is presented in Fig. 2. The models of aboveground live forest biomass varied by region in their ability to predict pixel-level values (Table 2). Correlation coefficients ranged from 0.92 in Puerto Rico down to 0.31 in the Southern region. The western regions had substantially better results than did those in the eastern regions of the US. Relative errors ranged from 0.51 in Puerto Rico to 0.92 in the Southern Region, with the former value indicating an approximate 50% improvement over using the sample mean from the model's training dataset, versus a more modest improvement in performance over a simple sample mean indicated by the latter value. Most individual mapping zones (75%) had relative errors less than 1.0, indicating gains in the modeling process. However, some zones actually had a relative error greater than 1.0 indicating the models performed worse than using a simple sample mean. This was particularly true in zones with a high proportion of scattered forest that is hard to identify with a 250 m pixel (e.g., zones 52, 44, and 49) and/or

Table 3
Assessment of agreement between plot-and map-based estimates of forest land area and total biomass over 4 scales of spatial aggregation across the continental US

Hexagon size (ha)	Estimate	Number of hexagons	Average plots/ hexagon	Proportion of hexagons				
				$-3<\tau$	$-3\leq\tau<-2$	$-2\leq\tau<2$	$2\leq\tau<3$	$\tau>3$
16,000	Forest area	25,512	9.40	0.013	0.011	0.938	0.026	0.012
21,000	Forest area	22,327	10.73	0.014	0.012	0.931	0.030	0.014
39,000	Forest area	15,993	14.99	0.019	0.019	0.908	0.036	0.018
65,000	Forest area	10,439	22.96	0.023	0.026	0.879	0.047	0.026
16,000	Biomass	25,512	9.40	0.003	0.007	0.887	0.042	0.061
21,000	Biomass	22,327	10.73	0.004	0.008	0.879	0.046	0.063
39,000	Biomass	15,993	14.99	0.005	0.012	0.860	0.049	0.074
65,000	Biomass	10,439	22.96	0.008	0.019	0.835	0.051	0.087

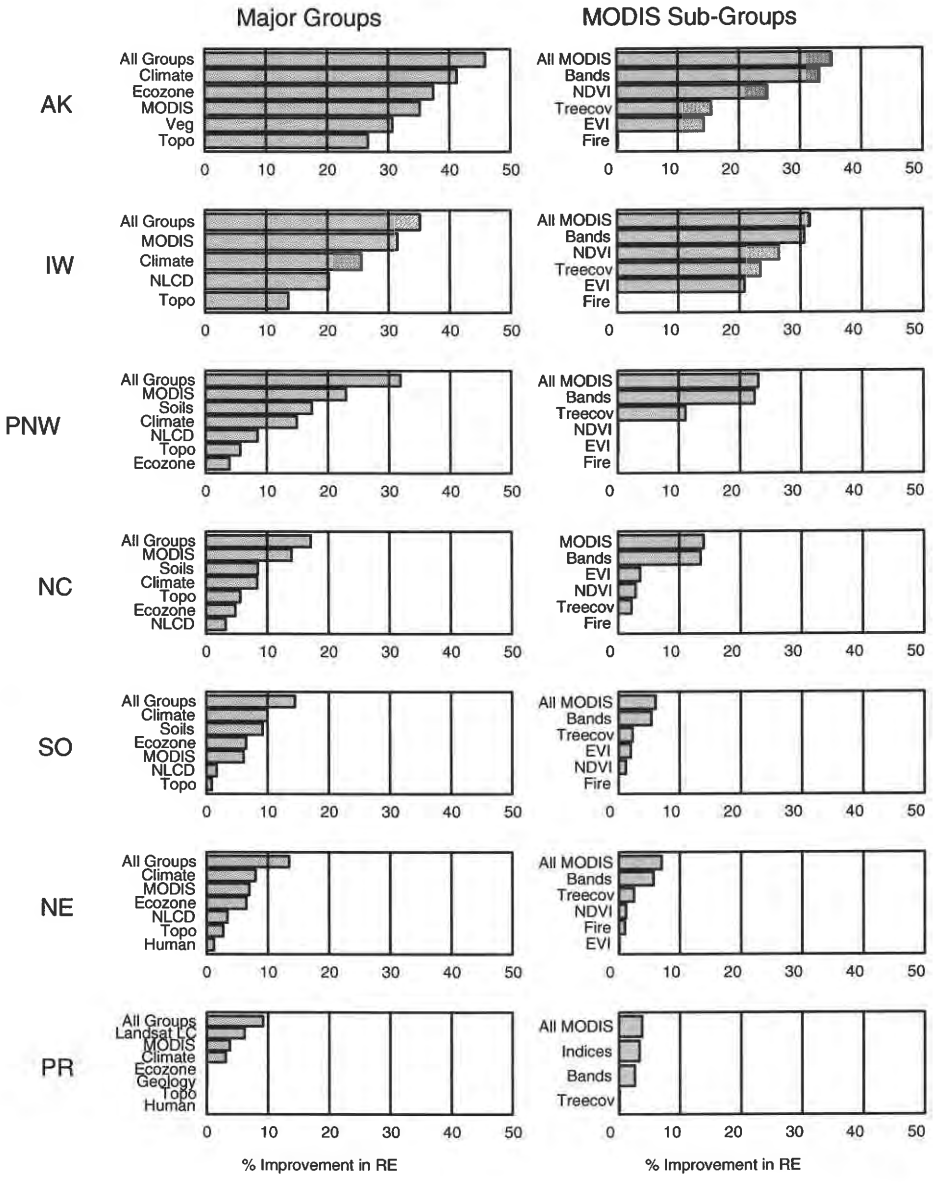

Fig. 5. Relative importance of the major groups of predictor variables as well as sub-groups of MODIS variables in each region. Importance is measured as the percent improvement in relative error when each variable group is used individually in a model of forest biomass. Regional abbreviations include: AK - Alaska, IW - Interior West, PNW - Pacific Northwest, NC - North Central, SO - Southern, NE - Northeast, and PR - Puerto Rico.

areas missing forest data (e.g., zones 32 and 35). Biomass model performance results are given for individual and aggregated zones in Appendix A.

3.2. Uncertainty maps

The forest probability map reflects uncertainty in pixel assignments to forest or nonforest categories in the forest mask. The forest probability map is a useful product of the forest-nonforest modeling process because it allows users to choose their own application-specific threshold for distinguishing between forested and nonforest lands. The biomass percent error map reflects uncertainty in the modeled pixel-level biomass values.

In general, the uncertainty maps reflect those areas that are more difficult to model because of their spatial characteristics, because of poor quality training or predictor data available in those areas, or because of a poor relationship between the desired response variable and the predictor layers available. In the forest probability map these were the interface areas between forest and nonforest, and in the forest biomass map these were the areas that were less intensely sampled, more affected by land use history (which was not an available predictor layer) or otherwise difficult to model.

Looking more closely at the resulting biomass, biomass uncertainty, and forest probability maps, regional differences in patterns of map uncertainty are apparent. In Fig. 3a, the Uinta Mountains of the Interior West, large areas of highly certain

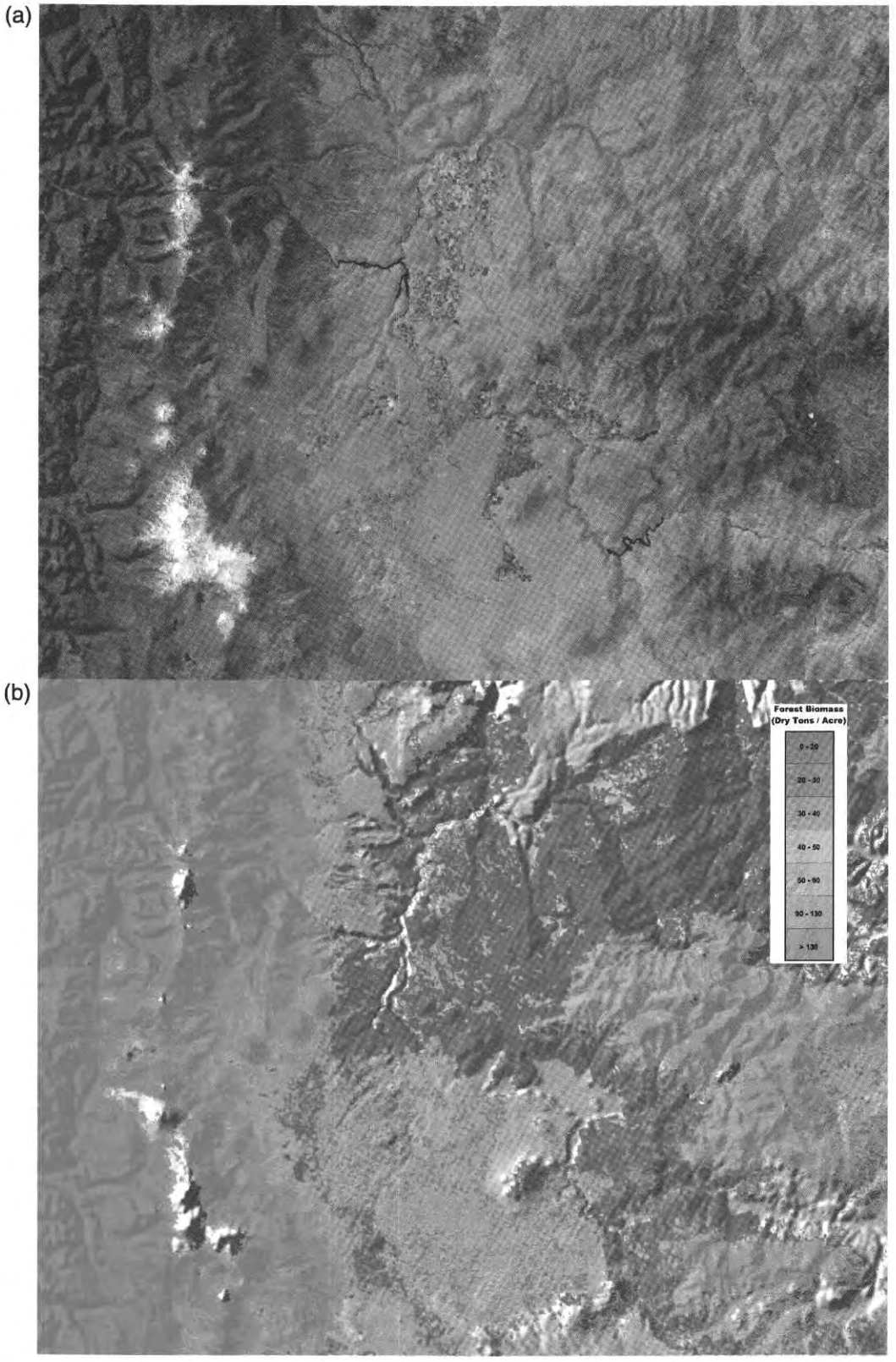

Fig. 6. An enlarged view of the natural color MODIS imagery (a), and the corresponding biomass dataset (b) from the Pacific Northwest in central Oregon.

nonforest exist relatively unbroken by pixels with much probability of forestland. In contrast, in the greater Mohawk Valley region of the Northeast (Fig. 3d), there are few continuous areas of highly certain nonforest.

In both regions it was the spatially heterogeneous areas that were the most difficult to predict — the highly intermixed forest-agriculture and forest-developed interfaces in the Northeast, and the sparse canopy transition zones between forest and nonforest

Table 4
Effect of excluding variable groups on relative error by region

Variable groups excluded	Increase in relative error						
	NE	NC	SO	INT	PNW	AK	PR
MODIS	0.01	0.04	0.03	0.02	0.05	0.03	0.02
Topo	0.00	0.00	0.01	0.01	0.01	0.02	−0.03
NLCD/Veg†	0.00	0.00	0.01	0.01	0.02	0.01	0.02
Climate	0.00	0.00	0.01	0.00	0.01	0.03	0.00
Soils/geology	–	0.01	0.01	–	0.02	–	0.00
Ecozone	0.00	0.01	0.01	–	0.01	0.01	−0.02
Human	0.00	–	–	–	–	–	0.00

†Land cover data for Puerto Rico from Helmer et al. (2002).
Increase in relative error is measured as the difference between relative error obtained excluding each of the major predictor groups in turn, and the relative error obtained using all the predictor variables.

areas at the elevational (i.e. treeline) and arid limits of tree growth in the Interior West. In both regions, the probability of forest values falling in the most uncertain range (0.4 to 0.6) represented just over 10% of the dataset — a substantial portion, illustrating the difficulty of accurately determining this edge, particularly at this resolution.

The uncertainties associated with biomass predictions in the Interior West are strongly related to the amount of biomass present, with higher percent errors associated with the lower biomass values (Fig. 3b). In the Northeast, percent errors were lower in general and show a spatial pattern that differs from the biomass predictions themselves (Fig. 3e). This pattern may reflect the distribution of different types of forest and our ability to model biomass in each, but also likely is the influence of the ancillary layers used in the modeling. Without the strong influence of a single variable, such as elevation, biomass predictions in the Northeast relied upon different predictor layers in different areas, each with varying levels of confidence that seemed to be visually correlated with these layers. Percent error values were in general much higher (above 0.8) in the Interior West (Fig. 3c) than in the Northeast (Fig. 3f). This is in large part due to the relatively lower biomass values present in the Interior West as compared to the Northeast.

3.3. Agreement of spatial aggregations

As described in Section 2.3.3, estimates of total forest area and biomass were computed by state from FIA sample plots. These plot-based estimates were compared to map-based estimates of total forest area and biomass that resulted from counting forested pixels and summing their biomass. At the state level, spatial aggregation results show fairly good agreement between the two sources for forest area, with notable exceptions in CO (where the map underestimates forest area) and GA, WV, NC, TX, and OK (where the map overestimates forest area). Twenty-nine of the states' map-based estimates fell within 10% of the plot-based estimates for forest area (Fig. 4a). For aboveground forest biomass, spatial aggregation results show an overestimation of biomass in most areas, with the notable exceptions of CA, OR, and WA where the map appears to substantially underestimate forest biomass. Substantial overestimation of state-level summaries appeared to occur in NC, VA, GA, AK, CA, OR, WA, and WV. Twenty one of the states' map-based estimates fell within 10% of the plot-based estimates for biomass (Fig. 4b).

Table 3 illustrates the distribution of τ-values to assess agreement between plot-and map-based estimates of total forest area and total biomass at four spatial scales of aggregation across the continental US. Map-based estimates of forest area generally were in agreement with plot-based estimates for all hexagon scales. However, spatial aggregations of hexagons with large absolute τ-values indicate that the forest mask is problematic in some portions of the Southeast; probably in parts of Maine, Wisconsin, Minnesota, Oklahoma, and along the Great Lakes; and perhaps in parts of the Pacific Coast states. These aggregations of hexagons with disagreeing estimates appear to be consistent across all four hexagon scales. Not surprisingly, the biomass map appears to exhibit more disagreement than observed for the forest mask at each hexagon aggregation. However, most disagreement in the biomass map resulted from over-estimates, while disagreement in the forest mask appeared more evenly distributed between over-estimates and under-estimates.

3.4. Variable importance

The first column in Fig. 5 depicts the relative importance of the major groups of predictor variables in each region. This was measured by percent improvement, or decrease, in relative error when each of these variable groups was used alone as predictor sets in different models of biomass. The bar labeled "All Groups" illustrates the maximum decrease in relative error obtained by including all the predictor variables, indicating improvement over just using the sample mean. In four of the seven regions (NC, IW, PNW, and PR), the "MODIS group" resulted in the largest improvement in relative error. In the other three regions (NE, SO,

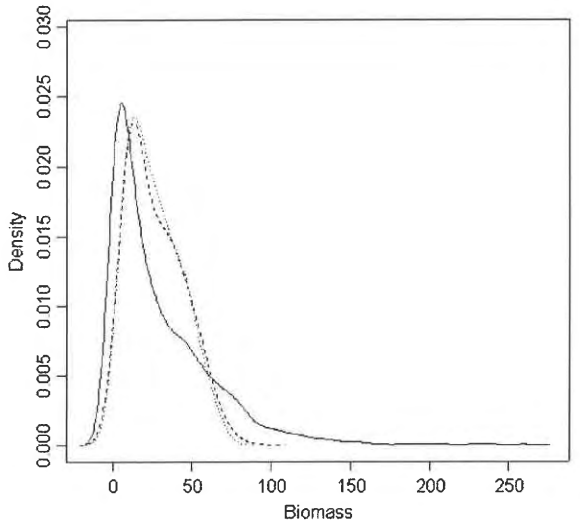

Fig. 7. The density function in the Interior West of observed biomass values (solid line), as compared to that from a model containing all the predictor variables (dashed line), and from a model excluding all the MODIS-derived variables (dotted line).

Table 5
Estimates of C pools in live forest biomass of continental U.S. forests

Source	Approach, spatial resolution, and study area addressed	Forest components	Forest biomass estimates for the U.S. (Pg C)[†]
Not spatially explicit			
Turner et al. (1995)	Inventory data by forest type at State level (1980–1990) for conterminous U.S.	Live trees, stumps, roots, branches, twigs and shrubs	14.96[‡]
Birdsey and Heath (1995)	Inventory data by forest type at State level (1980–1992) for continental U.S.	Live trees, stumps, roots, branches, twigs, shrubs and herbs	16.74
Spatially explicit			
Potter (1999)	Satellite-image scaled physiological model at 1° (1980s — ignores forest age structure) for the Earth	Live trees, stumps, roots, branches, twigs, and leaves.	37.65
Dong et al. (2003)	Inventory data at Province level scaled with satellite imagery to 8 km (1990–1995) for Northern Hemisphere temperate and boreal countries	Live trees, stumps, roots, branches, twigs and shrubs	12.48
This study	Inventory data at plot level scaled with satellite imagery to 250 m (2001) for continental U.S.[†]	Live trees, stumps, roots, branches and twigs	18.08[§]

[†]All estimates exclude Hawaii and Puerto Rico. This study estimates that Puerto Rican forests have 53.4 Mg C in aboveground live forest biomass.
[‡]Including 12.6 Pg C for conterminous U.S. plus 2.36 Pg C for Alaska from Birdsey and Heath (1995). [§]Includes root biomass estimated as 20% of total biomass (Cairns et al., 1997).

and AK) the "Climate group" resulted in the largest improvement in relative error. Use of just the "NLCD" and "Topo" groups alone resulted in smaller improvements in relative error than the "MODIS" or "Climate" groups in all regions. Some regions also opted to include additional variables groups related to soils, development, etc. Although not common to all regions, they are shown here for comparison sake. Note that because of high correlation between variables, the sum of decreases in relative error realized by modeling the groups individually cannot be expected to equal the total decrease in error when modeling all variables together. Variable groups contain redundant information, as will be illustrated later.

The second column in Fig. 5 depicts the relative importance of sub-groups of the MODIS-based variables as measured by percent improvement, or decrease, in relative error when each of these variable groups is used exclusively in the models. The bar labeled "All MODIS" provides a reference for the maximum decrease in relative error possible by using all the MODIS variables together. Using the "Bands" group alone (including all MODIS bands, all dates) resulted in models that performed nearly as well in most regions. Use of just the "NDVI" variables, "Treecov" (percent tree cover) variable, and "EVI" variables resulted in progressively smaller decreases in relative error. Note that the fire-related variables made no contribution when used alone. As with the major groups, sub-groups of variables within the MODIS group contain redundant information resulting in non-additivity of their relative contributions. Fig. 6a is an enlarged view of the natural color MODIS imagery, and the corresponding biomass dataset is shown in Fig. 6b. The image is from the Pacific Northwest in central Oregon, which visually demonstrates the high degree of correspondence between the MODIS data and biomass predictions.

While the results above illustrate the relative predictive information contained in each groups or sub-groups of variables, the true contribution of each variable to the final biomass map is confounded by high correlation between variables. Consequently, variable groups were excluded in turn from the original biomass model, and the effect on relative error shown in Table 4. In all cases except the MODIS group, exclusion of these variables resulted in a 2% or less change in relative error. Exclusion of the MODIS group had the largest impact over the other groups in all regions, although that impact, too, was very small, ranging from only 1% in the NE to 5% in the PNW. Also noted was the negative, albeit small, impact of including groups of variables exhibiting no contribution to the biomass prediction in Puerto Rico, where small sample size made models more vulnerable to extraneous information.

Not only was there minimal effect on pixel-level accuracies, the potential effect on pixel aggregations can be surmised by examining changes in density functions of predicted values under different models. Fig. 7 illustrates the density function in the Interior West of observed biomass values (solid line), as compared to that from a model containing all the predictor variables (dashed line), and from a model excluding all the MODIS-derived variables (dotted line). Both the all-variable model and the model excluding all the MODIS variables result in nearly identical densities. This illustrates the tendency in all these models to predict closely to the mean and not capture the observed variability in biomass. We also observed a very large discrepancy between variances for observed and variances for predicted values. As a side note, a likely contributor to this phenomenon is the spatial resolution (pixel size) at which the models are implemented. We only have biomass observations from small field plots and are modeling these to biomass on 250-m pixels. Yet we know that as pixel size increases, pixel values become more like the mean, and variance decreases. This will be addressed further in the discussion. But the differences between predicted value variances resulting from models excluding different groups of variables in turn are quite small. Because of redundancy of information between predictors, exclusion of any one of the major groups had only a small effect on the prediction accuracies and aggregations.

3.5. Estimates of C pools

Carbon pool estimates in live forest biomass of U.S. forests, derived from the map produced in this study, compare well with estimates from other studies (Table 5). The estimates for U.S. forests from Turner et al. (1995) and Birdsey and Heath (1995) are strictly plot-based (with the exception of Alaska), and they use FIA data from the 1980's to early 1990's. The estimate from Potter (1999) is from a global study and is high because it ignores forest age structure. It scales AVHRR NDVI data with a biophysical model, estimating potential forest biomass of forested areas. Dong et al. (2003) address temperate and boreal forests of the Northern Hemisphere. They scale state-and province-level estimates of total forest biomass from forest inventory data with cumulative NDVI indices from AVHRR data. It is the smallest estimate for around 1990 and may indicate that using satellite imagery to scale state-level forest biomass underestimates forest biomass. These forest carbon estimates probably also differ because the scales of these studies range from national to global.

4. Discussion

Image products from MODIS were useful for this study not only because they were practical, but also because they were preferable for scaling reasons. From a practical standpoint, the coarser spatial resolution of MODIS imagery makes applications at sub-continental scales computationally less intensive compared with finer resolution data. Moreover, MODIS image products, like tree cover data and preprocessed image composites that minimize cloud cover, along with the larger scene and tile sizes, reduce the burdens of image preprocessing. At the same time, the land imaging MODIS bands include optical bands comparable to finer scale data. These bands center on visible, near infrared and shortwave infrared bands that many studies show are sensitive to forest cover and, within limits, forest stand structure. Bands 1 and 2 of MODIS, for instance, are centered on the red and near infrared parts of the electromagnetic spectrum and are important in indices sensitive to photosynthetic vegetation. Bands 2 and 6 are similar to Landsat image bands 4 (near infrared) and 5 (shortwave infrared), respectively, which form indices sensitive to forest structure or successional stage in both temperate (Fiorella & Ripple, 1993) and tropical (Helmer et al., 2000) landscapes.

From a scaling perspective, the 250 to 500-m pixel size of MODIS bands 1–2 and 3–7, respectively, were beneficial overall. Variable importance analyses revealed that MODIS-derived information could contribute more predictive power than other classes of information when used in isolation. However, because of strong correlation between variables, the true contribution of MODIS-derived variables when used in concert with the broad suite of other predictors was quite small. In addition, the coarse scale likely added to plot-pixel differences. A summary of possible sources of per-pixel errors in the biomass map would include: 1) reflectance values in dense canopy forests saturate at relatively low levels of forest biomass, 2) the spatial mismatch between the FIA plots and the 250-m pixels, and 3) errors in the forest/nonforest mask. With 250-m pixels, positional inaccuracy is unlikely to contribute to model errors, though it could be a factor.

First we address the saturation of reflectance values. In most mapping zones, the models tended to underestimate large biomass densities and overestimate small ones, truncating the range of values predicted and adding to the average relative error in models. The most important source of these residual errors in mapping models probably stems from the well-known fact that canopy reflectance from passive optical sensors has limited sensitivity to the canopy structure of dense forests, where most live forest biomass is. Forests continue to accumulate biomass after canopies close as well as after indices of vegetation greenness and net primary production level off. Yet this very limitation was one of the reasons why we worked at a spatial resolution of 250 m. The advantage of 250-m pixels is that less forestland is captured as fully forested pixels that are more likely to saturate pixel reflectance, and more forestland is captured within partially forested, spatially coarse pixels that reflect both forest and nonforest cover. This advantage provides a novel explanation of why modeling at coarser spatial scales improves per-pixel estimates of forest stand or canopy attributes. Studies report that errors for per-pixel estimates of forest volume and biomass decline from over 50% to 10–12% as 20 to 30-m pixels are aggregated to larger pixels of 19 ha (Reese et al., 2002) and up to 360 ha (Kennedy et al., 2000). Models of leaf area index also improve when aggregating pixels from 30 m to 500–1000 m (Cohen et al., 2003). Our own preliminary analyses revealed that biomass model correlations decreased if we increased the minimum fraction of forest area in the pixels that were included in a model.

In fact, we propose that tree or forest cover can relate to forest biomass density of a pixel in two ways. First, mass balance tells us that for uniform forest, the forest biomass density of a pixel is directly proportional to forest cover. By assuming that each pixel within the forest mask is fully forested, biomass density becomes a function of tree or forest cover for a uniform forest. Secondly, and in addition to simple mass balance, more fragmented forest or forest adjacent to nonforest (and associated with less surrounding tree or forest cover) is more likely to be disturbed or young (Helmer, 2000), have less biomass per ha of forest (Brown et al., 1993; Laurance et al., 1997), and have lower mean canopy heights (E. Helmer, unpublished data). Under this scenario, tree or forest cover data are among the most important predictor variables where forest cover is less than about 60%. A clear strength of the MODIS tree cover product, then, is that it is a global product that explains significant variance in forest biomass when data range from low to high tree cover. The weakness of proportional tree or forest cover is that these variables reach their maximums before forest biomass does. For example, the MODIS-derived tree cover product explains 37% of the variance in mean forest canopy heights across the Amazon basin where tree cover is at least 20% (N=3828), but only 1.6% of the variance in mean forest canopy heights where it is at least 60% (N=2734). Mean canopy heights for forest with at least 60% or 75% tree cover do not significantly differ (Helmer & Lefsky, 2006; E. Helmer, unpublished data).

A second potential source of per-pixel error is the spatial mismatch between the size of an FIA plot, which is distributed

over 0.67–2.5 ha (depending on region of the country), and the larger, 250-m pixels that extend over 6.25 ha. This situation, where a single FIA plot may not represent the average of the surrounding 6 ha, could inflate error estimates where local variability in forest biomass is high (for biomass estimates) and/or land cover heterogeneity is high (for forest/nonforest estimates). If so, the model errors from these site-specific assessments may conservatively gauge pixel-level errors in biomass densities. This effect of spatial mismatch on model performance measures has been noted by others (Congalton & Plourde, 2000; Foody, 2002; Smith et al., 2003; Verbyla & Hammond, 1995).

A third potential source of error is that pixels with less than 0.5 predicted probability of forest were considered 'nonforest' and received no biomass estimates, even though they could contain forest cover and biomass. Likewise, pixels having more than 0.5 predicted probability forest were considered forest. This tendency to underestimate forest area in sparsely forested regions, and overestimate it in heavily forested ones, is well documented for thematic land cover classifications of coarse spatial resolution pixels (Kuusela & Päivinen, 1995; Mayaux & Lambin, 1995; Nelson, 1989). Furthermore, FIA plot-based estimates pertain to forest land use, while satellite image-based estimates portray forest land cover. FIA definitions of forest land use and land cover are equivalent in many, but not all areas. For example, a change from forest cover to nonforest cover occurs when harvest, wildfire, windstorm, or other events result in removal of standing live trees. Such treeless areas still are defined as forest land use, assuming that regeneration is expected to occur and other land uses are not intended. Conversely, some areas having extensive tree cover are defined as nonforest use, due to other prevailing uses of the land, e.g., treed picnic areas, parks, and golf courses. In addition, effective differences in definition exist between what is observed and inventoried on the ground (e.g. total aboveground tree biomass; tree-covered residential areas) and what is captured by a satellite-borne optical sensor (e.g. tree biomass visible from above). Thus, some apparent discrepancies between plots and pixels, and resulting decreases in model accuracies, may, in fact, be artifacts of definitional inconsistencies between land use and land cover, and differences between ground inventory and optical satellite perspectives. Independent efforts are being initiated to assess these discrepancies, including use of non-FIA datasets for pixel accuracy and error and demographic data for differentiating land use from land cover.

Not surprisingly, a closer correspondence was observed between spatial aggregations of statewide map-based estimates and FIA plot-based estimates than between per-pixel comparisons with individual plots. These results are like those of Muukkonen and Heiskanen (2005) who reported large estimation errors of forest stand biomass, but spatially aggregated map-based estimates of forest biomass were comparable to municipality-level estimates from Finland's National Forest Inventory. With regard to scales of aggregation, model-based estimates of forest proportion and forest biomass tended to agree with plot-based estimates at all four scales tested. This is interesting in that despite sometime extremely high per-pixel percent errors for biomass, spatial aggregations can still provide reasonable estimates. This may be due to the fact that the per-pixel accuracy assessment is negatively impacted by the fact that the plot, which is taken to characterize the entire pixel, is very small in size relative to the size of the pixel, and furthermore it is only a single sample from the pixel. This negative effect is ameliorated to some degree by the "averaging effects" of the larger area of the hexagons; i.e., some of the errors from cancel each other.

For some geographic locales, however, particularly for the biomass map, hexagon aggregations with large absolute τ-values raise concerns over the utility of the map in those specific areas. This lack of consistency is not surprising, given the variability in ecological conditions, image data, and plot data across the US. Many of those states with the largest differences between the plot-based and map-based estimates of forest biomass and forest area are states where the most recent available data were from an older periodic inventory, or where data were not available statewide, or where poor GPS coordinates or other conditions made modeling particularly difficult. In addition, some of the differences observed may also reflect differences in definition (total aboveground tree biomass versus tree biomass visible from satellite-borne optical sensors). A relationship also exists between the difference in the estimates for forest land and the difference in estimates for forest biomass, implying that improvements in the initial forest/nonforest mask, or use of a different cutoff in the forest probability map, might increase compatibility between plot-and map-based estimates in some areas.

Presenting uncertainty maps in conjunction with the nationwide forest biomass map emphasizes that the biomass estimates are somewhat imprecise and that their uncertainty varies by location. It is important to include this uncertainty information in assessing the reliability of model-based estimates of forest area and biomass. The map-based estimates of nationwide total live above ground biomass yield estimates of total forest C storage that are within the range of previous map- and plot-based estimates of C storage or biomass, and they are consistent with the consensus that forests in the Northern hemisphere are a net C sink (Pacala et al., 2001; Schimel et al., 2001).

Zone discrepancies still exist in the current final map of aboveground forest biomass presented here. Considerable effort went in to compiling and screening the FIA data, however some areas were still handicapped by holes in the available data (e.g. zones 26, 32, 34, 35, and 36 in TX and OK), out-of-date plot data in an area of rapid change (much of the Southeast), and low quality GPS coordinates for the FIA plots (several states in the Southeast). These show up in the current map as distinct lines between zones where one side of the line may have been modeled with local but inaccurate data, and the other side of the line was modeled with more accurate but more distant data requiring an extrapolation of the model into the area of interest. This project, among others, highlights the important effects on mapping of both quantity and quality of FIA plot data, and the high value of improving such data. The current efforts within FIA including the shift to annual inventory, complete coverage with GPS and consistent data collection protocols nationwide

should substantially alleviate these problems for future modeling efforts.

5. Conclusions

Spatially explicit forest biomass information at the scale of the US provides an unprecedented picture of how forest biomass is distributed spatially across US landscapes and permits visual assessment of forest biomass distribution. It synthesizes point data from tens of thousands of ground plots into one spatial dataset that can easily feed into those ecosystem and atmospheric models that do not assimilate the point-based data. The accuracy assessments reflect the understanding that the data are primarily useful for coarse-scale modeling. The accompanying spatially explicit datasets of model uncertainty provide information critical to estimating uncertainty in such atmospheric, ecosystem, or other models and estimates (Brown et al., 1993; Brown & Schroeder, 1999; Canadell et al., 2000; Dong et al., 2003; Nemani et al., 2003; Potter, 1999). Nationwide spatially explicit modeling of forest characteristics with ground-based inventory data presented logistical and institutional challenges. Although overcoming those challenges required extensive national coordination, it forged an institutional process for nationwide forest attribute mapping that benefited from regional expertise.

Appendix A. Per-pixel measures of performance for forest/nonforest maps based on independent test sets, by zone within regions

Mapping zone	PCC	Kappa	Sensitivity	Specificity	Test set sample size
Northeast					
52	0.91	0.18	0.18	0.97	160
60	0.86	0.69	0.73	0.94	154
61	0.88	0.73	0.91	0.82	171
62	0.86	0.71	0.88	0.82	104
63	0.84	0.62	0.9	0.71	70
64	0.76	0.36	0.83	0.54	55
65	0.88	0.73	0.95	0.75	139
66	0.95	0.52	0.99	0.45	328
Northcentral					
30, 31	0.98	0.56	0.50	0.99	1613
33, 38, 43	0.94	0.50	0.54	0.97	848
41	0.89	0.78	0.92	0.87	754
44	0.86	0.80	0.86	0.94	696
47	0.80	0.53	0.65	0.87	221
49	0.95	0.82	0.80	0.98	299
50	0.90	0.80	0.90	0.90	632
51	0.89	0.78	0.84	0.93	735
Interior West					
10	0.92	0.59	0.99	0.49	525
12	0.94	0.72	0.75	0.97	883
13	0.96	0.50	0.58	1.00	121
14	0.93	0.10	0.08	0.99	220
15	0.83	0.63	0.88	0.75	338
16	0.75	0.42	0.92	0.47	298
17	0.89	0.69	0.74	0.94	397
18	0.94	0.38	0.35	0.98	413
19	0.92	0.84	0.93	0.91	410
20	0.96	0.41	0.32	0.99	535
21	0.88	0.75	0.91	0.84	245
22	0.97	0.42	0.28	1.00	466
23	0.8	0.48	0.62	0.87	332
24	0.89	0.68	0.73	0.94	486
25	0.89	0.54	0.52	0.96	366
27	0.92	0.50	0.47	0.97	287
28	0.82	0.64	0.87	0.77	292
29	0.95	0.66	0.62	0.98	582
Pacific Northwest					
1	0.89	0.63	0.95	0.63	3245
2	0.89	0.75	0.93	0.81	1832
3	0.88	0.74	0.91	0.83	1949
4	0.97	0.69	0.65	0.99	3442
5	0.99	0.00	0.00	1.00	2150
6	0.87	0.74	0.87	0.87	2406
7	0.85	0.71	0.89	0.82	2981
8	0.97	0.54	0.45	0.99	1457
9	0.87	0.54	0.56	0.94	5464
Southern					
26, 32, 36	0.96	0.86	0.86	0.99	188
34	–	–	–	–	0
35	–	–	–	–	0
37	0.88	0.73	0.93	0.79	410
45	0.88	0.66	0.65	0.96	216
46	0.81	0.43	0.90	0.59	594
47	0.87	0.71	0.78	0.83	149
48	0.85	0.69	0.93	0.74	119
53	0.87	0.64	0.93	0.69	106
54, 59	0.86	0.35	0.95	0.35	156
55	0.88	0.59	0.92	0.70	197
56	0.67	0.39	0.61	0.73	63
57	0.83	0.38	0.96	0.35	93
58	0.86	0.35	0.97	0.30	118
Alaska	0.94	0.88	0.93	0.95	6553
Puerto Rico	0.79	0.57	0.93	0.64	28

Appendix A (*continued*)

Appendix B. Per-pixel measures of performance for biomass maps based on independent test sets, by zone within region

Mapping zone	Average absolute error	Relative error	Correlation coefficient	Test set sample size
Northeast				
52	88.3	1.39	0.17	19
60	63.2	0.82	0.53	65
61	65.0	0.97	0.32	133
62	64.5	0.95	0.39	171
63	67.8	0.93	0.44	159
64	57.0	0.91	0.40	195
65	60.4	0.95	0.22	142
66	49.7	0.73	0.33	272
Northcentral				
30, 31, 29, 40, 42	43.0	0.85	0.39	51
33, 38, 43	40.8	0.98	0.35	50
44, 49	44.4	1.03	0.12	347

Appendix B (*continued*)

Mapping zone	Average absolute error	Relative error	Correlation coefficient	Test set sample size
Northcentral				
41	40.6	0.90	0.44	313
50	44.1	0.87	0.47	308
51	46.0	0.90	0.45	197
Interior West				
10	66.0	0.81	0.57	468
12, 13, 14	17.1	0.90	0.31	123
15	26.1	0.58	0.71	230
16	39.9	0.76	0.57	203
17, 18	22.4	0.86	0.48	103
19	52.0	0.84	0.46	207
20, 29	34.5	0.72	0.59	80
21	50.4	0.75	0.59	134
22, 23	24.4	0.76	0.68	105
24	17.9	0.74	0.69	114
25, 27	18.0	0.64	0.71	85
28	39.9	0.68	0.63	171
Pacific Northwest				
1	132.6	0.81	0.51	529
2	157.1	0.88	0.46	169
3	144.8	0.84	0.52	146
4, 5	93.1	0.93	0.28	45
6	119.2	0.76	0.49	267
7	116.6	0.69	0.57	535
8, 9	51.58	0.85	0.45	289
Southern				
26, 32, 36	26.8	1.02	0.20	17
34	-	-	-	0
35	-	-	-	0
37	54.7	0.96	0.26	256
45	40.7	0.86	0.35	48
46	63.5	0.93	0.25	414
47	65.5	1.05	0.14	94
48	56.6	0.96	0.24	67
53	62.5	0.89	0.31	82
54	51.7	1.06	0.08	119
55	64.6	0.95	0.28	159
56	94.6	0.74	0.39	26
57	59.7	0.97	0.38	73
58	117.6	0.89	0.34	138
59	87.2	0.96	0.39	96
Alaska	91.5	0.59	0.69	430
Puerto Rico	65.0	0.51	0.92	*

Average absolute error is reported in metric tons per hectare. *10-fold cross-validaton.

References

Bauer, E., & Kohavi, R. (1998). An empirical comparison of voting classification algorithms: bagging, boosting, and variants. *Machine Learning*, *5*, 1–38.

Bechtold, W. A., & Patterson, P. L., (Eds). (2005). *The Enhanced Forest Inventory and Analysis Program—National Sampling Design and Estimation Procedures*. General Technical Report GTR-SRS-080. Asheville, NC: U.S. Department of Agriculture, Forest Service, Southern Research Station.

Birdsey, R., & Heath, L. (1995). Carbon changes in U.S. forests. In L. Joyce (Ed.), *Productivity of America's forests and climate change* (pp. 56-70). Fort Collins, CO: USDA Forest Service General Technical Report RM-271, Rocky Mountain Forest and Range Experiment Station.

Breiman, L. (1996). Bagging predictors. *Machine Learning*, *26*, 123–140.

Breiman, L. (1998). Arcing classifiers (with discussion). *Annals of Statistics*, *26*, 801–849.

Breiman, L., Friedman, J. H., Olshen, R. A., & Stone, C. J. (1984). *Classification and regression trees*. Monterey, CA: Wadsworth and Brooks/Cole.

Brown, S. L., Iverson, L. R., & Lugo, A. (1993). Land use and biomass changes of forests in peninsular Malaysia during 1972–1982: use of GIS analysis. In V. H. Dale (Ed.), *Effects of Land Use Change on Atmospheric CO2 Concentrations: South and Southeast Asia as a Case Study* (pp. 117–143). New York: Springer-Verlag.

Brown, S., & Lugo, A. E. (1992). The storage and production of organic matter in tropical forests and their role in the global carbon cycle. *Biotropica*, *Vol. 14*, 161–187.

Brown, S. L., & Schroeder, P. E. (1999). Spatial patterns of aboveground production and mortality of woody biomass for eastern U.S. forests. *Ecological Applications*, *9*, 968–980.

Cairns, M. A., Brown, S., Helmer, E., & Baumgardner, G. (1997). Root biomass allocation in the world's upland forests. *Oecologia*, *111*, 1–11.

Canadell, J. G., Mooney, H. A., Baldocchi, D. D., Berry, J. A., Ehleringer, J. R., Field, C. B., et al. (2000). Carbon metabolism of the terrestrial biosphere: a multi-technique approach for improved understanding. *Ecosystems*, *3*, 115–130.

Chan, J. C. W., Huang, C., & DeFries, R. S. (2001). Enhanced algorithm performance for land cover classification using bagging and boosting. *IEEE Transactions on Geoscience and Remote Sensing*, *39*(3), 693–695.

Cochran, W. G. (1977). *Sampling Techniques*. New York: Wiley.

Cohen, J. (1960). A coefficient of agreement of nominal scales. *Educational and Psychological Measurement*, *20*, 37–46.

Cohen, W. B., Maiersperger, T. K., Yang, Z., Gower, S. T., Turner, D. T., Ritts, W. D., et al. (2003). Comparisons of land cover and LAI estimates derived from ETM+ and MODIS for four sites in North America: a quality assessment of 2000/2001 provisional MODIS products. *Remote Sensing of Environment*, *88*(3), 233–255.

Congalton, R. G., & Plourde, L. C. (2000). Sampling methodology, sample placement, and other important factors in assessing the accuracy of remotely sensed forest maps. In G. B. M. Heuvelink & M. J. P. M. Lemmens (Eds.), *Proceedings of the 4th International Symposium on Spatial Accuracy Assessment in Natural Resources and Environmental Sciences* (pp. 117–124). The Netherlands: Delft University Press.

Daly, C. (2002). *PRISM monthly and annual precipitation and temperature for Alaska*. Climate Source LLC.

Daly, C., Helmer, E. H., & Quiñones, M. (2003). Mapping the climate of Puerto Rico, Vieques and Culebra. *International Journal of Climatology*, *23*, 1359–1381.

Daly, C., Kittel, T., McNab, A., Gibson, W., Royle, J., Nychka, D., et al. (2000). Development of a 103-year high-resolution climate data set for the conterminous United States. *Proceedings of the 12th AMS Conference on Applied Climatology* (pp. 249–252). Asheville, NC: American Meteorological Society.

Dong, J., Kaufmann, R. K., Myneni, R. B., Tucker, C. J., Kauppi, P. E., Liski, J., et al. (2003). Remote sensing estimates of boreal and temperate forest woody biomass: carbon pools, sources, and sinks. *Remote Sensing of Environment*, *84*, 393–410.

Edwards, T. C., Jr., Cutler, D. R., Zimmermann, N. E., Geiser, L., & Moisen, G. G. (2006). Effects of sample survey design on the accuracy of classification models in ecology. *Ecological Modelling*, *199*, 132–141.

Fan, S., Gloor, M., Mahlman, J., Pacala, S., Sarmiento, J., Takahashi, T., et al. (1998). A large terrestrial carbon sink in North America implied by atmospheric and oceanic carbon dioxide data and models. *Science*, *282*, 442–446.

Fiorella, M., & Ripple, W. J. (1993). Determining successional stage of temperate coniferous forests with Landsat satellite data. *Photogrammetric Engineering and Remote Sensing*, *59*, 239–246.

Foody, G. M. (2002). Status of land cover classification accuracy assessment. *Remote Sensing of Environment*, *80*, 185–201.

Fortin, M., Edwards, G. & Thomson, K. P. B. (1999). The role of error propagation for integrating multisource data within spatial models: the case of the DRASTIC groundwater vulnerability model. In K. Lowell A. Jaton (Eds.), Spatial Accuracy Assessment-Land Information Uncertainty in

Natural Resources (pp. 437-443). Chelsea, MI: Sleeping Bear Press/Ann Arbor Press.

Freund, Y., & Schapire, R. (1996). Experiments with a new boosting algorithm. In L. Saitta (Ed.), *Machine Learning: Proceedings of the Thirteenth International Conference* (pp. 148–156). San Fransisco, CA: Morgan Kauffman.

Gesch, D., Oimoen, M., Greenlee, S., Nelson, C., Steuck, M., & Tyler, D. (2002). The national elevation dataset. *Photogrammetric Engineering and Remote Sensing*, *68*, 5–11.

Hansen, M., DeFries, R., Townshend, J. R., Carroll, M., Dimiceli, C., & Sohlberg, R. (2003). *500 m MODIS Vegetation Continuous Fields: Tree Cover.* College Park, MD: GLCF, University of Maryland.

Helmer, E. H. (2000). The landscape ecology of secondary forest in montane Costa Rica. *Ecosystems*, *3*, 98–114.

Helmer, E. H., Cohen, W. B., & Brown, S. (2000). Mapping montane tropical forest successional stage and land use with multi-date Landsat imagery. *International Journal of Remote Sensing*, *21*, 2163–2183.

Helmer, E. H., Lefsky, M. (2006). Forest canopy heights in Amazon River basin forests as estimated with the Geoscience Laser Altimeter System (GLAS). In Aguirre-Bravo, C. Pellicane, Patrick J. Burns, Denver P. & Draggan, Sidney, eds. 2006. Monitoring Science and Technology Symposium: Unifying Knowledge for Sustainability in the Western Hemisphere. 2004 September 20-24; Denver, CO. Proceedings RMRS-P-37CD. Fort Collins, CO: U.S. Department of Agriculture, Forest Service, Rocky Mountain Research Station. CD-ROM.

Helmer, E. H., Ramos, O., Lopez, T. D. M., Quiñones, M., & Diaz, W. (2002). Mapping forest types and land cover of Puerto Rico, a component of the Caribbean biodiversity hotspot. *Caribbean Journal of Science*, *38*, 165–183.

Holland, E. A., Brown, S., Potter, C. S., Klooster, S. A., Fan, S., Gloor, M., et al. (1999). North American carbon sink. *Science*, *283*, 1815.

Homer, C. G., & Gallant, A. (2001). *Partitioning the conterminous United States into mapping zones for Landsat TM land cover mapping.* USGS Draft White Paper available at http://landcover.usgs.gov

Houghton, R. A. (1999). The annual net flux of carbon to the atmosphere from changes in land use 1850-1990. *Tellus*, *51B*, 298–313.

Houghton, R. A. (2003). Revised estimates of the annual net flux of carbon to the atmosphere from changes in land use and land management 1850–2000. *Tellus*, *55B*, 378–390.

Huete, A., Didan, K., Miura, T., Rodriguez, E., Gao, X., & Ferreira, L. (2002). Overview of the radiometric and biophysical performance of the MODIS vegetation indices. *Remote Sensing of Environment*, *83*, 195–213.

Justice, C. O., Townshend, J. R. G., Vermote, E. F., Masuoka, E., Wolfe, R. E., Saleous, N., et al. (2002). An overview of MODIS Land data processing and product status. *Remote Sensing of Environment*, *83*, 3–15.

Kennedy, P., Folving, S., Estreguil, M., Rosengren, E., Tomppo, E., Pereira, J. M., et al. (2000). Forest information from remote sensing — biomass and wood volume assessment and mapping. In T. Zawila-Niedzwiecki (Ed.), *Proceedings of the 4.02.05 Group Session; Remote Sensing and World Forest Monitoring (held within IUFRO XXI World Congress on Forests and Society, pp. 17–32).* Warsaw: Institute of Geodesy and Cartography.

Kuusela, K., & Päivinen, R. (1995). On the classification of ecosystems in boreal and temperate forests. In P. J. Kennedy, R. Päivinen, & L. Roihuvuo (Eds.), *Proceedings of an International Workshop Designing a System of Nomenclature for European Forest Mapping*, (pp. 387-393). Joensuu, Finland: Institute for Remote Sensing Applications, Joint Research Centre, European Commission and the European Forest Institute.

Laurance, W., Laurance, S., Ferreira, L., Rankin-de Merona, J., Gascon, C., & Lovejoy, T. (1997). Biomass collapse in Amazonian forest fragments. *Science*, *278*, 1117–1118.

Mayaux, P., & Lambin, E. F. (1995). Estimation of tropical forest area from coarse spatial resolution data: a two-step correction function for proportional errors due to spatial aggregation. *Remote Sensing of Environment*, *53*, 1–15.

Miles, P. D., Brand, G. J., Alerich, C. L., Bednar, L. F., Woudenberg, S. W., Glover, J. F., et al. (2001). The forest inventory and analysis database: database description and users manual version 1.0. *General Technical Report NC-218.* St. Paul, MN: U.S. Department of Agriculture, Forest Service, North Central Research Station 130 pp.

Moisen, G. G., Freeman, Blackard, J., Frescino, T. S., Zimmermann, N. E., & Edwards, T. C. (2006). Predicting tree species presence in Utah: a comparison of stochastic gradient boosting, generalized additive models, and tree-based methods. *Ecological Modelling*, *199*, 176–187.

Moisen, G. G., & Frescino, T. S. (2002). Comparing five modeling techniques for predicting forest characteristics. *Ecological Modelling*, *157*, 209–225.

Mowrer, H. T. (1994). Monte Carlo techniques for propagating uncertainty through simulation models and raster-based G.I.S. In R. G. Congalton (Ed.), *Proceedings of the International Symposium on the Spatial Accuracy of Natural Resource Data Bases* (pp. 179–188). Bethesda, MD: American Society of Photogrammetry and Remote Sensing.

Muukkonen, P., & Heiskanen, J. (2005). Estimating biomass for boreal forests using ASTER satellite data combined with standwise forest inventory data. *Remote Sensing of Environment*, *99*, 434–447.

Nelson, R. (1989). Regression and ratio estimators to integrate AVHRR and MSS data. *Remote Sensing of Environment*, *30*, 201–216.

Nemani, R. R., Keeling, C. D., Hashimoto, H., Jolly, W. M., Piper, S. C., Tucker, C. J., et al. (2003). Climate-driven increases in global terrestrial net primary production from 1982 to 1999. *Science*, *300*, 1560–1563.

Pacala, S. W., Hurtt, G. C., Baker, D., Peylin, P., Houghton, R. A., Birdsey, R. A., et al. (2001). Consistent land-and atmosphere-based U.S. carbon sink estimates. *Science*, *292*, 2316–2320.

Potter, C. S. (1999). Terrestrial biomass and the effects of deforestation on the global carbon cycle. *Bioscience*, *49*, 769–778.

Potter, C., Klooster, S., Genovese, V., & Myneni, R. (2003). Satellite data helps predict terrestrial carbon sinks. *EOS Transactions, American Geophysical Union*, *Vol. 84*, 502–508.

Prentice, I. C., Farquhar, G. D., Fasham, M. J. R., Goulden, M. L., Heimann, M., Jaramillo, V. J., et al. (2001). The carbon cycle and atmospheric carbon dioxide. In D. Yihui (Ed.), *Climate change 2001: The scientific basis* (pp. 183–237). Cambridge, UK: Cambridge University Press.

Quinlan, J. R. (1986). Induction of decision trees. *Machine Learning*, *1*, 81–106.

Quinlan, J. R. (1993). *C4.5: Programs for Machine Learning.* San Mateo, CA: Morgan Kaufman Publishers.

Reese, H., Nilsson, M., Sandström, P., & Olsson, H. (2002). Applications using estimates of forest parameters derived from satellite and forest inventory data. *Computers and Electronics in Agriculture*, *37*, 37–55.

Särdnal, C. E., Swensson, B., & Wretman, J. H. (1992). *Model Assisted Survey Sampling.* New York: Springer-Verlag.

Schimel, D. S., House, J. I., Hibbard, K. A., Bousquet, P., Ciais, P., Peyline, P., et al. (2001). Recent patterns and mechanisms of carbon exchange by terrestrial ecosystems. *Nature*, *414*, 169–172.

Scott, C. T., Bechtold, W. A., Reams, G. A., Smith, W. D., Hansen, M. H., & Moisen, G. G. (2005). Sample-based estimators used by the forest inventory and analysis national information management system. In W. A. Bechtold P.L. Patterson (Eds.), *The Enhanced Forest Inventory and Analysis Program—National Sampling Design and Estimation Procedures. Gen. Tech. Rep. SRS-80.* Asheville, NC: U.S. Department of Agriculture, Forest Service, Southern Research Station.

Smith, J. H., Stehman, S. V., Wickham, J. D., & Yang, L. M. (2003). Effects of landscape characteristics on land-cover class accuracy. *Remote Sensing of Environment*, *84*, 342–349.

Thompson, M. E. (1997). *Theory of Sample Surveys.* London: Chapman and Hall.

Turner, D., Koerper, G., Harmon, M., & Lee, J. (1995). A carbon budget for forests of the conterminous United States. *Ecological Applications*, *5*, 421–436.

Valliant, R., Dorfman, A. H., & Royall, R. M. (2001). *Finite population sampling and inference: a prediction approach.* New York: Wiley.

Verbyla, D. L., & Hammond, T. O. (1995). Conservative bias in classification accuracy assessment due to pixel-by-pixel comparison of classified images with reference grids. *International Journal of Remote Sensing*, *16*, 581–587.

Vermote, E. F., & Vermueulen, A. (1999). *Atmospheric correction algorithm: spectral reflectances (MOD09).* College Park, MD: University of Maryland.

Vogelmann, J. E., Howard, S., Yang, L., Larson, C., Wylie, B., & Van Driel, N. (2001). Completion of the 1990s National Land cover Data set for the

conterminous United States from Landsat Thematic Mapper data and ancillary data sources. *Photogrammetric Engineering and Remote Sensing, 67*, 650–661.

White, D., Kimerling, A. J., & Overton, W. S. (1992). Cartographic and geometric components of a global sampling design for environmental monitoring. *Cartography and Geographic Information Systems, 19*(1), 5–22.

Woodbury, P. B., Smith, J. E., Weinstein, D. A., & Laurence, J. A. (1998). Assessing potential climate change effects on loblolly pine growth: A probabilistic regional modeling approach. *Forest Ecology and Management, 107*, 99–116.

Global Change Biology

Targeting current species ranges and carbon stocks fails to conserve biodiversity in a changing climate: opportunities to support climate adaptation under 30x30

Journal:	*Global Change Biology*
Manuscript ID	Draft
Wiley - Manuscript type:	Primary Research Articles
Date Submitted by the Author:	n/a
Complete List of Authors:	Dreiss, Lindsay; Defenders of Wildlife, Center for Conservation Innovation Lacey, L; Defenders of Wildlife, Center for Conservation Innovation Weber, Theodore; Defenders of Wildlife, Department of Landscape Conservation Delach, Aimee; Defenders of Wildlife, Department of Landscape Conservation Niederman, Talia; Defenders of Wildlife, Center for Conservation Innovation Malcom, Jacob; Defenders of Wildlife, Center for Conservation Innovation
Keywords:	climate refugia, climate corridors, protected areas, biodiversity conservation, carbon mitigation
Abstract:	Protecting areas for climate adaptation will be essential to ensuring greater opportunity for species conservation well into the future. However, many proposals for protected areas expansion focus on our understanding of current spatial patterns, which may be ineffective surrogates for future needs. A science-driven call to address the biodiversity and climate crises by conserving at least 30% of lands and waters by 2030, 30x30, presents new opportunities to inform the siting of new protections globally and in the U.S. Here we identify climate refugia and corridors based on a weighted combination of currently available models; compare them to current biodiversity hotspots and carbon-rich areas to understand how 30x30 protections siting may be biased by data omission; and compare identified refugia and corridors to the Protected Areas Database to assess current levels of protection. Available data indicate that 20.5% and 27.5% of identified climate adaptation areas (refugia and/or corridor) coincides with current imperiled species hotspots and carbon-rich areas, respectively. With only 12.5% of climate refugia and corridors protected, a continued focus on current spatial patterns in species and carbon richness will not inherently conserve places critical for climate adaptation. However, there is ample opportunity for establishing future-minded protections: 52% of the contiguous U.S. falls into the top quartile of values for at least one class of climate refugia. Nearly 27% is already part of the protected areas network, but managed for multiple uses that may limit their ability to contribute to the goals of 30x30. Additionally, nearly two-thirds of

	nationally identified refugia coincide with ecoregion-specific refugia suggesting representation of nearly all ecoregions in national efforts focused on conserving climate refugia. Based on these results, we recommend that land planners and managers make more explicit policy priorities and strategic decisions for future-minded protections and climate adaptation.

Title

Targeting current species ranges and carbon stocks fails to conserve biodiversity in a changing climate: opportunities to support climate adaptation under 30x30

Authors

Lindsay M. Dreiss[1]*, L. Mae Lacey[1], Theodore C. Weber[2], Aimee Delach[2], Talia E. Niederman[1], Jacob W. Malcom[1]

Affiliations

[1]Center for Conservation Innovation, Defenders of Wildlife, Washington, DC 20036, USA.

[2]Department of Landscape Conservation, Defenders of Wildlife, Washington, DC 20036, USA.

***Correspondence**

Lindsay Dreiss, Defenders of Wildlife 1130 17th Street NW, Washington, DC 20036

lrosa@defenders.org, 202.772.3201

ABSTRACT

Protecting areas for climate adaptation will be essential to ensuring greater opportunity for species conservation well into the future. However, many proposals for protected areas expansion focus on our understanding of current spatial patterns, which may be ineffective surrogates for future needs. A science-driven call to address the biodiversity and climate crises by conserving at least 30% of lands and waters by 2030, 30x30, presents new opportunities to inform the siting of new protections globally and in the U.S. Here we identify climate refugia and corridors based on a weighted combination of currently available models; compare them to current biodiversity hotspots and carbon-rich areas to understand how 30x30 protections siting may be biased by data omission; and compare identified refugia and corridors to the Protected Areas Database to assess current levels of protection. Available data indicate that 20.5% and 27.5% of identified climate adaptation areas (refugia and/or corridor) coincides with current imperiled species hotspots and carbon-rich areas, respectively. With only 12.5% of climate refugia and corridors protected, a continued focus on current spatial patterns in species and carbon richness will not inherently conserve places critical for climate adaptation. However, there is ample opportunity for establishing future-minded protections: 52% of the contiguous U.S. falls into the top quartile of values for at least one class of climate refugia. Nearly 27% is already part of the protected areas network, but managed for multiple uses that may limit their ability to contribute to the goals of 30x30. Additionally, nearly two-thirds of nationally identified refugia coincide with ecoregion-specific refugia suggesting representation of nearly all ecoregions in national efforts focused on conserving climate refugia. Based on these results, we recommend that land planners and managers make more explicit policy priorities and strategic decisions for future-minded protections and climate adaptation.

Keywords: Climate refugia, Climate corridors, Protected areas, Biodiversity conservation, Carbon mitigation

INTRODUCTION

The spatial heterogeneity of shifting climatic conditions presents challenges and opportunities for large-scale biodiversity conservation, as impacts to habitat and species can vary significantly across the landscape (Baldwin et al. 2018). In North America, nearly half of species are already undergoing local extinctions (Wiens 2016), which are, in part, due to increasing temperatures and decreasing precipitation (Roman-Palacios and Wiens 2020). In the contiguous U.S. (CONUS), the average annual temperature has risen 1.2-1.8 °C since the beginning of the 20th century, with the largest net increases occurring in western regions (Vose et al. 2017). Precipitation patterns are also shifting, with increases in central and northern United States and large reductions in the Southeast and West (Fei et al. 2017, Wuebbles et al. 2017). As the effects of climate change accelerate, local biodiversity will either need to adapt or make effective use of the changing landscape; species may find locations that serve as refugia from extreme or rapid climatic changes or shift their ranges to better-suited habitat (Neilson et al. 2005, Keppel and Wardell-Johnson 2012, Franks and Hoffman 2012, Román-Palacios and Wiens 2020). Identifying and conserving important refugia habitats and dispersal routes will be one critical step in jointly addressing the biodiversity and climate crises for the longer term (Pörtner et al. 2021). Therefore, it is important to understand what conservation planning opportunities exist in those areas where climate shifts are less extreme or more stabilized. While expansion of the U.S. protected areas network has been identified as an important solution to lowering extinction risk and overall ecosystem degradation (Stolton et al. 2015, Gray et al. 2016, Dinerstein et al 2017, 2019), efforts generally focus on present species distributions and may not effectively reflect future needs (Elsen et al. 2020, Maxwell et al. 2020).

Calls to address the joint biodiversity and climate crises by protecting at least 30% of Earth by 2030, known as "30x30" (Dinerstein et al. 2019), have been endorsed by government and conservation leaders at global (United Nations 2020), national (Biden 2021, U.S. DOI et al. 2021), and state levels (e.g., Newsom 2020). While the specifics of carrying out such a plan have yet to be established (Büscher et al. 2016, Rights and Resources Initiative 2020, Simmons et al. 2021), efforts would hypothetically conserve areas needed to sustain essential ecological services and reverse extinction trends (Locke 2013, Dinerstein et al. 2017). Translating these commitments into national policy may prove challenging since the protected areas network is

incongruous with locations that could effectively maximize biodiversity conservation (Scott et al. 2001, Jenkins et al. 2015, Venter et al. 2018) or climate mitigation (Buotte et al. 2019, Melillo et al. 2015). However, it is unclear how well the current network and 30x30 goals can ensure the conservation of climate-resilient habitat in the coming decades as climate change continues to accelerate.

Climate-resilient habitat can largely be delineated into refugia and corridors. Generally, refugia protect native species and ecosystems from negative effects of climate change in the short term by remaining relatively buffered from climatic changes over time (Morelli et al., 2020). For example, steep canyons and north-facing slopes are sheltered from solar radiation and heat accumulation (Stralberg et al., 2020a) and wet areas like wetlands and riparian zones can remain moist during droughts (Morelli et al., 2016; Stralberg et al., 2020a). Refugia can be identified by various approaches which rely on at least one of three main concepts: topodiversity, climate exposure, and climate tracking (Michalak et al. 2020). Topodiversity models are based on physical habitat data and highlight regions with varied land cover, climate, soil, and topographic conditions, which may produce microrefugia (Ackerly et al. 2010, Groves et al. 2012, Carroll et al. 2018). Climatic exposure models are based on projected climatic changes and represent the degree of climate change likely to be experienced by a species or locale (Saxon 2011, Groves et al. 2012). Lastly, climate tracking models are based on one or more representative climate models and measure the proximity and accessibility of future suitable climatic conditions (Hamann et al. 2015, Michalak et al. 2018).

However, to survive in the face of ongoing and worsening climate change impacts, species may need to disperse longer distances to adapt and find more suitable habitat (Roman-Palacios and Wiens 2020). Climate corridors are relatively climate-stable areas that can facilitate long-distance dispersal (Stralberg et al., 2020b) by connecting current and future habitat. Network theory principles can be used to model climate corridors by delineating single paths or diffuse flow between climate analogs. Depending on model inputs, corridors may emphasize movement toward cooler latitudes and topographies, along rivers and streams, and/or through areas providing better habitat and less stress from disturbances (McGuire et al. 2016, Stralberg 2020b, Carroll et al. 2018, Littlefield et al. 2017).

Given the urgency of the biodiversity and climate crises, there is a pressing need to

include potential climate refugia and corridors in the conservation planning process. However, some challenges exist. First, a growing body of available spatial data for identifying areas important for climate adaptation means that planners must reconcile a diversity of data (Carroll and Ray 2021). Previous research indicates that identified priority areas can be highly dependent on the datasets used as each represents different mechanisms and highlights different landscapes (Michalak et al. 2020, Carroll and Ray 2021). Second, the majority of prioritization frameworks for protected areas expansion focus on current spatial patterns in biodiversity, landscape connectivity and other key factors (Cushman et al. 2009, Lookingbill et al. 2010, Dickson et al. 2013, Belote et al. 2016, McClure et al. 2016). Focusing on the current state of the environment may result in critical omissions in protected areas siting for longer-term persistence of some target species (Monzón et al. 2011, Elsen et al. 2020). If this is the case, consideration of future conditions may complement efforts to preserve current biodiversity and ecosystem service hotspots, thereby reducing the threat of mass extinctions and accompanying biosphere degradation. Last, other omissions may occur if identification and prioritization of areas for climate resilience happen at a national scale: national-level analyses do not necessarily provide adequate representation of all natural ecoregions, communities, and species (e.g. Kraus and Hebb). Taking additional steps to identify refugia at multiple scales may help increase ecosystem representation and protections for the unique species assemblages and services they harbor.

Proper identification, protection, and management of climate-informed refugia and corridors are essential to ensuring greater opportunity for species conservation via migration and adaptation. While previous research and policy discussion surrounding the protected areas network has identified areas important to conserving the current state of biodiversity and natural carbon storage (Scott et al. 2001, Myers et al. 2000, Gray et al. 2016, Buotte et al. 2020), to our knowledge, there are no analyses of coincidence of these with areas important to species climate adaptation. To help close this knowledge gap, we:

1. identify areas in the contiguous U.S. critical to climate adaptation based on coincidence and complementarity among refugia (national and ecoregion-specific) and corridors models;
2. compare the spatial distribution of identified climate refugia and corridors with current biodiverse and carbon-rich areas; and

3. quantify the extent to which climate refugia and corridors are considered protected.

Step #2 guides our understanding of how protections siting under the 30x30 framework may be biased by data omission, and step #3 helps to assess the current level of protection for identified climate refugia and distinguish where stronger management might be needed. Our research contributes to a growing literature demonstrating the importance of incorporating climate-informed data in place-based land protection policy and practices and helping to identify specific areas for conservation. While these analyses are not meant to serve as a map of priority lands for conservation, they help frame a discussion on operationalizing 30x30 for strategic, future-minded conservation decisions.

METHODS

For this analysis, we focus on spatial datasets based on climate models or topography to identify areas that could serve as important refugia or migration routes for the contiguous U.S. (CONUS; Table 1). All datasets using climate models are informed by an ensemble of three to seven General Circulation Models (GCMs) for emission scenario Representative Concentration Pathway (RCP) 4.5 and projected for the time period 2071-2100. RCP 4.5 requires that carbon dioxide (CO_2) emissions start declining by approximately 2045 to reach roughly half of the levels of 2050 by 2100 (IPCC 2014). Recent studies suggest that near-term CO_2 emissions - an indicator of likely outcomes under current policies - agree more closely with RCP 4.5 than more extreme scenarios (e.g., RCP 8.5, International Energy Agency 2019, Hausfather and Peters 2020). All datasets have been resampled and aligned at 1km resolution. We combined datasets for refugia (n = 8) and corridors (n = 2) separately, accounting for differences in underlying mechanisms in modeling method and landscape conservation principles.

Climate refugia

We initially analyzed relationships between datasets through a principal components analysis where each component helps define a refugia class. As with principal components, datasets were assigned to a class based on the sign and size of the eigenvector. However, to avoid a tradeoff in refugia identification within a single class, all datasets within the class were required to load together and in the same direction on a principal component. In addition to

presenting three separate classes, we weighted datasets based on their principal component loadings and combined them in a single dataset so that no one refugia class has a greater weight in identifying climate refugia locations. All datasets were normalized to a scale of 0 to 1 prior to being combined. Based on the relationships between refugia datasets, the weighted combination was calculated as:

$$Combined\ Refugia = Z_{Bird\ Macrorefugia} + Z_{Current\ Climate\ Diversity} + Z_{Ecotypic\ Diversity} + Z_{Land\ Facet\ Diversity} + Z_{Landscape\ Diversity} + (Z_{Climatic\ Dissimilatiry} * 2.5) + (Z_{Climate\ Velocity} * 2.5) + (Z_{Tree\ Macrorefugia} * 5)$$

We analyzed locations in the 80th percentile (i.e., the top 20% of values) of the distribution of values for the combined data and for each refugia class separately. Additionally, we quantified the degree of overlap in refugia classes.

In addition to CONUS-level analyses, we extracted refugia values for each ecoregion separately (EPA level II; EPA 2006), classifying the locations that fell into the top 20% of the distribution as areas of interest. The result was a map of ecoregion-specific refugia, ensuring equal representation of all ecoregions relative to size. Results from the national- and ecosystem-scale analyses were compared and contrasted using spatial overlays.

Climate corridors

We extracted raw data values on connectivity and climate flow (The Nature Conservancy 2020) for areas that were identified as 'climate-informed' corridors based on the categorical connectivity and climate flow dataset (The Nature Conservancy 2020). The remaining values were rescaled to fall between 0 and 1. A second climate corridor dataset (Carroll et al. 2018) was similarly rescaled. We then combined these two datasets and analyzed locations in the 80th percentile of the distribution of combined values.

Analyses

We used spatial overlay analysis to describe the extent to which the current protected areas network covers identified climate refugia (based on national- and ecoregion-scales) and corridors in CONUS. We quantified the extent to which identified refugia would be protected by the 30x30 framework if it were to solely focus on current areas of high imperiled species

biodiversity and ecosystem carbon. Data on protected areas are from the PADUS 2.1 database (USGS 2020). We use U.S. Geological Survey's Gap Analysis Program (GAP) codes, which are specific to the management intent to conserve biodiversity. GAP 1 and 2 areas are managed in ways typically consistent with conservation. Areas assigned a GAP 3 code are governed under multiple-use mandates that may include biodiversity priorities but may also include incompatible activities such as forestry and mining, and GAP 4 areas lack any conservation mandates or such information is unknown as of 2020. As such, GAP codes are a natural system for identifying possible policy paths to achieving 30x30 and advancing wildlife conservation in the United States. Imperiled species richness was assessed from publicly available range data (USGS GAP, International Union of Conservation of Nature - IUCN, and U.S. Fish and Wildlife Service) for species defined as 'imperiled' (1,923 species). These include species that are listed or under consideration for listing under the ESA, have a NatureServe G1-3 status and/or are in critically endangered, endangered or vulnerable IUCN categories. Modeled total ecosystem carbon is based on a high-resolution map of global above- and below-ground carbon stored in biomass and soil (Soto-Navarro et al. 2020). We used ArcPro v2.5 (ESRI, USA) to produce maps and run analyses, with maps using the Albers Equal Area Conic projection. All area statistics are based on GIS estimates using this projection.

RESULTS

Identifying refugia and corridors

Climate refugia datasets generally correlated well with others of similar methodology or concept; three resulting classes generally represent topodiversity, climatic stability, and tree macrorefugia (Tables 1 & S1). The main exception was for climate-based datasets with species information, where bird macrorefugia correlated with datasets based on topodiversity, but tree macrorefugia was the sole dataset in its class (Table S2). The three refugia classes exhibited very little overlap with one another at the national scale: while 52% of CONUS falls into at least one of the refugia classes, 7.5% falls into refugia identified by 2 or more classes (approx. 568,000 km^2, Fig. S1). Additionally, two classes (tree macrorefugia and climatic stability) were strongly and negatively correlated with one another. Locations in the combined refugia layer that were within the top 20% of the distribution of values represent these overlaps and are used for reporting the remainder of statistics here.

34% of CONUS is identified as a climate refugia or corridor under one or more datasets (approx. 2,652,000 km^2, Fig. 1). Climate refugia generally follow the Appalachian, Rocky, and Cascade Mountain Ranges with additional refugia in the Ozarks, Ouachitas, southern Sierra Nevadas and along the California coast. Climate corridors are somewhat complementary to national-scale refugia, with 28.9% of their area (444,501 km^2) overlapping identified refugia locations. Overlaps occur in the central Appalachians, Pacific Northwest, and portions of the Rockies, Sierra Nevadas and Ozarks. Corridors that do not overlap with refugia are key in connecting parts of the Great Plains and Mexico borderlands to refugia and in connecting refugia to northern locales, particularly in New England, Midwest, Crown of the Continent and between northern California and the Cascades.

Using a stratified ecoregion approach resulted in refugia that were highly coincident with lands identified in the national scale analysis, with 63% of all national refugia overlapping with ecoregion refugia (Fig. 2). Overlaps between the two cover 12% of CONUS total land area (approx. 949,000 km^2). All refugia combined (both from national and ecoregion-specific analyses) equal 26% of the total CONUS land area (approx. 2.1 million km^2). Locations that were emphasized in the ecoregion-specific approach include temperate and semi-arid prairies and places along the eastern coast.

Comparison to 30x30 objectives: biodiversity and carbon

Refugia and corridors are generally complementary on the landscape to areas of current high biodiversity and carbon storage values (Fig. 3a&b). There is some overlap between current biodiversity hotspots (i.e., top quartile of imperiled species richness values) and identified national-scale refugia (36.8%) and corridors (9.3%; Table 2). Overlaps are generally concentrated in western California and Appalachia/Ozarks regions. Overlap between carbon-rich areas is greater in extent overall (refugia overlap = 32.5% and corridor overlap = 27.2%) and similar in spatial pattern with greater overlap in northern areas: northern Appalachians, Crown of the Continent and Pacific Northwest. When combining the two objectives (biodiversity and/or carbon), 45.0% (approx. 1,000,000 km^2) of the land area representing at least one of these objectives is also identified as part of a climate refuge or corridor.

Taking an ecoregion-specific approach to comparing refugia, corridors, biodiversity, and carbon results in less coincidence in current and future values: 22.0% and 21.7% of stratified refugia overlap with ecoregion-specific biodiversity hotspots and carbon-rich areas, and 17.5% and 26.1% of corridors overlap with ecoregion-specific biodiversity hotspots and carbon-rich areas, respectively (Fig. 3c&d; Table 3).

Current protections for refugia and corridors

Overall, 12.5% of the combined network of refugia and corridors is managed consistently with biodiversity conservation (i.e., GAP 1 or 2; 4.2% of CONUS or approx. 325,000 km^2; Fig. 4). The rest of this network falls on GAP 3 (26.5%) or GAP 4 (69.3%) lands, which represents 29.2% of CONUS (approx. 2,280,000 km^2). Proportions are similar when analyzing protection of national-scale climate refugia and corridors separately (Table 2). Ecoregion-specific refugia fall more heavily in GAP 4 categories with 12.2% of area on lands managed for biodiversity conservation and 19.6% on those managed for multiple uses (Fig. 4, Table 3). Finally, the entire set of CONUS lands representing either biodiversity conservation (GAP 1 or 2) or 30x30 objectives (biodiversity hotspots and/or carbon-rich areas) coincides with 44.5% of the national climate refugia and corridor network.

DISCUSSION

Currently, the U.S. protected areas network and emerging conservation policy objectives largely fail to represent valuable climate refugia and corridors. While there is some overlap with 30x30 objectives, solely using recent imperiled species ranges and carbon stores as conservation criteria will not inherently protect climate-resilient lands. In the most protective situation - if all biodiversity hotspots and carbon-rich areas were to be considered for strong conservation mandates (e.g., GAP 1 or 2 protections) - a majority (55.5%) of identified climate refugia or corridors would still be left unprotected. The omission of landscapes for climate adaptation from planning initiatives could inhibit the potential for longer-term conservation successes. As decision makers evaluate protected areas expansion, it will be important to prioritize lands and waters that will allow species to adapt and persist in a changing climate. While simply protecting

currently biodiverse or carbon-rich areas may not ensure the preservation of climate corridors and refugia, conserving corridors and refugia will benefit imperiled species in biodiversity-rich hotspots and promote carbon sequestration. This is particularly true in parts of the country (e.g., Appalachia and western California) where hotspots are not directly covered by climate corridors, but adjacent to them, providing opportunities for migration to refugia or future climate analogs.

With over half of the contiguous U.S. identified as at least one type of climate refugia (topodiversity, climatic stability, or tree macrorefugia), many opportunities exist for decision makers interested in future-minded conservation. Our analysis supports previous work suggesting potential trade-offs in using one refugia type over other in refugia identification: approaches based on topodiversity favor environmentally complex regions, whereas climatic exposure and tree macrorefugia highlight lands beyond mountain ranges and areas of similar complexity (Michalak et al. 2020). Through our ensemble approach to refugia identification we both highlight the complementary information provided by these approaches (Belote et al. 2018) and simplify varied complex datasets for greater interpretability. A weighted combination of the datasets puts less pressure on the user to choose between mechanisms and on the decision maker to have a deep understanding of the methodology when interpreting maps. However, clarification of a specific refugia type may help states or local municipalities working at varying scales to set different priorities for contributing to national refugia protections based on local environments and community needs. In addition, taking a combined approach results in high overlap with an ecoregion-stratified approach, suggesting representation of nearly all ecoregions in national efforts focused on conserving climate refugia.

Currently unprotected climate refugia and corridors represent 29.2% of CONUS, of which 38% is federally managed. Given the extent and distribution of land managers, protecting valuable climate adaptation areas can help contribute to the 30% target numerically and meaningfully. However, there will need to be a concerted effort by land managers in all jurisdictions and leadership across jurisdictional boundaries.

Lands Administered by Government and Tribal Entities

Public lands can make significant contributions to achieving 30x30. The federal lands estate is particularly expansive (20% of CONUS, 86% of PADUS; CRS 2020, Rosa and Malcom

2020) and federal land management agencies are required to varying degrees to prioritize wildlife and habitat conservation. Currently, the majority (86%, representing 18.4% of CONUS) of GAP 3 lands are managed by federal agencies, suggesting that substantial gains can be made in focusing on existing statutory authorities to advance climate-smart conservation on these lands. Refugia with GAP 3 coverage present abundant opportunities to strengthen management mandates for climate adaptation, also adding to achievability of full linkage protection. Of GAP 3 lands, over half are managed by the Bureau of Land Management (BLM) and another third by the U.S. Forest Service (Rosa and Malcom 2020). Both agencies are guided by multiple use management mandates that empower them to designate and manage lands to enhance protection of areas recognized as having important conservation values (respectively, the Federal Land Policy and Management Act of 1976, National Forest Management Act of 1976). The agencies can capitalize on existing land and water designation authorities - like wilderness designation and BLM "areas of critical environmental concern" - to increase protection for climate refugia and corridors.

Expansion of GAP 1 and 2 lands to cover more refugia and corridors can also ensure greater conservation for climate adaptation. The U.S. Fish and Wildlife Service manages the National Wildlife Refuge System (NWRS) to conserve and restore wildlife, fish, and plants and their native habitats. Because refuge lands are expressly managed to conserve species and habitat, they offer a high level of federal land protection. Pursuing the acquisition of lands fundamental to species' survival and sustainability, including climate refugia and climate corridors, to establish new refuges would be consistent with the purview of NWRS, future-minded conservation and 30x30 objectives. However, since federal land acquisition and management decisions are often politically contentious, this may be a less feasible option for conserving the additional 440 million acres of land needed to reach the 30% target.

State governments also manage significant acreage (approximately 4% of the U.S.), including state forests, wildlife management areas, game lands, and natural area preserves. State parks, or portions thereof, may also contribute to conservation refugia and corridors, but are often categorized as GAP 4 (i.e., absent or unknown mandates for conservation). States can contribute to 30x30 by upgrading GAP status and management of undeveloped state lands that can contribute to climate adaptation. Furthermore, through the State Wildlife Action Planning

(SWAP) process, each state is required to describe "locations and relative condition of key habitats and community types essential to conservation of species" (USFWS & AFWA 2017). Results from this and other studies can help inform this process, and be a resource as states increasingly update their SWAPs to include climate changes (NFWPCAN 2021).

Tribal nations hold over 56 million acres in trust by the Bureau of Indian Affairs and may manage their lands in ways that afford more substantive protections for lands and species given their lower rates of habitat modification (Lee-Ashley et al. 2019). As many indigenous peoples are deeply connected to local culturally important resources such as plant and animal species, they are also impacted by climate-driven alterations in ecosystem processes and biodiversity (Jantarasami et al. 2018). A long history of managing and observing their lands has provided many indigenous communities with valuable knowledge and experience to inform land management and planning for climate adaptation and resilience (BIA 2018). Respectful inclusion of indigenous systems of knowledges and perspectives "can inform our understanding of how the climate is changing and strategies to adapt to climate change impacts" (NFWPCAN 2021). As such, government-to-government relationships will be important in addressing climate adaptation needs for species and peoples and may include cross-landscape management, tribal involvement in federal and state planning, and more. The Landscape Conservation Cooperative (LCC) program developed by Interior offers one such mechanism to advance landscape-scale protections and coordinate climate-related land conservation activities among Tribal Nations, federal agencies, state, local, and tribal governments, and other stakeholders (NASEM 2016).

Private and Non-Governmental Organization Lands

As most land in the United States is privately owned, conservation efforts on private lands will be critical to expanding protected areas. 62% of the refugia and 56% of corridors fall outside of the protected areas network (GAP 4), but this only represents 20% of CONUS. This suggests that well-targeted, voluntary acquisitions and easements could translate to large gains in private lands conservation. Land trusts are uniquely positioned to scale up conservation on private lands to achieve the 30x30 target and, when strategic with land protections, help protect these areas and fill important gaps in the nation's 30x30 network.

In addition to the role of land trusts, private working lands also have an important role to play in achieving 30x30 (Garibaldi et al. 2020, American Farmland Trust 2021). The Farm Bill conservation programs administered by the U.S. Department of Agriculture will be particularly important to achieving these goals (Theoharides 2014). For instance, the Agriculture Conservation Easement Program (ACEP) could be targeted to lands identified as climate refugia or connectivity areas and specify sensitive wetland habitats and riparian areas as eligible lands for wetland easements, as these will be increasingly valuable for supporting wildlife and ecosystem services as the climate changes (Theoharides 2014, Lewis et al. 2019). Longer-term (30 year) ACEP contracts that offer a commitment to consider re-enrollment of the same or similar land at contract expiration should be encouraged to ensure enduring conservation measures. Additionally, Environmental Quality Incentives Program (EQIP) and the Conservation Stewardship Program (CSP) can better reflect climate adaptation needs by assigning higher ranking points practices designed to build resilient natural resources, promote ecosystem services, and increase the adaptive capacity of the entire agro-ecosystem to climate change (Theoharides 2014).

Limitations

In order to enhance species' resilience in the face of growing climate and biodiversity crises, corridors and refugia must be preserved across both lands and waters. Due to some limitations of data and our analyses, we recommend against siting protections based on the coincidence of current biodiversity/carbon hotspots and climate refugia/corridors alone. For one, complementarity of species assemblages is not accounted for in using species richness. As a result, there may be biases toward conserving certain taxa. Additionally, while we included aquatic species in our biodiversity metric, and wetland/riparian areas are part of some topographic measures of refugia/corridors, we did not explicitly include aquatic refugia. At this time, there is no complete national dataset to represent aquatic refugia. Because cold-water aquatic organisms like salmon, trout, hellbenders, spring salamanders, and various macroinvertebrates are among the most vulnerable taxa to climate change, future analyses should focus on identifying freshwater refugia and corridors in regions where sufficient data exists (e.g., brook trout refugia in the northeast U.S. (Letcher et al., 2017), stream temperature scenarios in the western U.S. (Isaak et al., 2016), and Springs Online (https://springsdata.org), a collaborative

database of spring locations and spring-dependent species in the Western U.S. and northern Mexico). Like terrestrial refugia, protection and restoration (where needed) of these areas should be focused at multiple scales, including protecting recharge areas, forests, and wetlands in the watershed (Stranko et al., 2008; Doyle and Shields, 2012; Jayakaran et al., 2016; Merriam et al., 2019), and restoring floodplains, riparian buffers and stream geomorphology (Sullivan and Watzin, 2009; Sweeney and Newbold, 2014; Favata et al., 2018; Merriam et al., 2019). Given the international scope of 30x30 and the benefits of larger-scale connectivity, future work on climate adaptation in 30x30 implementation should look beyond terrestrial habitats and political boundaries to cover all ecosystems of North America.

Our analysis demonstrates the need to make climate adaptation a more explicit objective in conservation planning for addressing the biodiversity crisis. Without direct consideration for climate refugia and corridors, a 30x30 implementation focused on current species ranges and carbon stocks may be ineffective for the longer term persistence of species. The key to operationalizing 30x30 and subsequent efforts will be growing a protected areas network that ensures a long-term commitment to biodiversity and climate. By incorporating climate refugia and corridors, the U.S. can work to protect places that will continue to serve wildlife and human populations now and in the future.

ACKNOWLEDGEMENTS

We thank M. Anderson, J. Grand, J. Lawler, R. List, J. Michalak, S. Saunders, and R. Wynn-Grant for their thoughtful review of the project and engaging discussion over key concepts. Additional gratitude goes to those organizations that make these datasets publicly available to enable this and other research.

DATA AVAILABILITY

The data that support the findings of this study are all publicly available. Those directly generated by this work can be downloaded from the following OSF repository: https://osf.io/jksyx/

LITERATURE CITED

Ackerly, D. D., Loarie, S. R., Cornwell, W. K., Weiss, S. B., Hamilton, H., Branciforte, R., & Kraft, N. J. B. (2010). The geography of climate change: Implications for conservation biogeography: Geography of climate change. *Diversity and Distributions*, *16*(3), 476–487. https://doi.org/10.1111/j.1472-4642.2010.00654.x

AdaptWest Project. (2015). Gridded climatic velocity data for North America at 1km resolution. https://adaptwest.databasin.org/pages/adaptwest-velocitywna/

American Farmland Trust. (2021). Agriculture's Role in 30x30: Partnering with Farmers and Ranchers to Protect Land, Biodiversity, and the Climate. American Farmland Trust. https://s30428.pcdn.co/wp-content/uploads/2021/04/AFT_-_Agricultures_Role_in_30x30_-_4-5-2021.pdf

Baldwin, R. F., Trombulak, S. C., Leonard, P. B., Noss, R. F., Hilty, J. A., Possingham, H. P., Scarlett, L., & Anderson, M. G. (2018). The Future of Landscape Conservation. *BioScience, 68(2)*, 60–63. https://doi.org/10.1093/biosci/bix142

Belote, R. T., Dietz, M. S., McRae, B. H., Theobald, D. M., McClure, M. L., Irwin, G. H., McKinley, P. S., Gage, J. A., & Aplet, G. H. (2016). Identifying Corridors among Large Protected Areas in the United States. *PLOS ONE, 11(4)*, e0154223. https://doi.org/10.1371/journal.pone.0154223

Belote, R. T., Carroll, C., Martinuzzi, S., Michalak, J., Williams, J. W., Williamson, M. A., & Aplet, G. H. (2018). Assessing agreement among alternative climate change projections to inform conservation recommendations in the contiguous United States. *Scientific Reports*, *8*(1), 9441. https://doi.org/10.1038/s41598-018-27721-6

Biden, J.R. (2021). Executive Order on Tackling the Climate Crisis at Home and Abroad. https://www.whitehouse.gov/briefing-room/presidential-actions/2021/01/27/executive-order-on-tackling-the-climate-crisis-at-home-and-abroad/

Buotte, P. C., Law, B. E., Ripple, W. J., & Berner, L. T. (2020). Carbon sequestration and biodiversity co-benefits of preserving forests in the western United States. *Ecological Applications, 30(2),* https://doi.org/10.1002/eap.2039

Bureau of Indian Affairs (BIA). (2018). National Climate Assessment: Indigenous Peoples' Resilience Actions. https://biamaps.doi.gov/nca/

Büscher, B., Fletcher, R., Brockington, D., Sandbrook, C., Adams, W. M., Campbell, L., Corson, C., Dressler, W., Duffy, R., Gray, N., Holmes, G., Kelly, A., Lunstrum, E., Ramutsindela, M., & Shanker, K. (2017). Half-Earth or Whole Earth? Radical ideas for conservation, and their implications. *Oryx, 51(3),* 407-410.https://doi.org/10.1017/S0030605316001228

Carroll, C., Roberts, D.R., Michalak, J.L. et al. (2017). Scale-dependent complementarity of climatic velocity and environmental diversity for identifying priority areas for conservation under climate change. Global Change Biology Early View. https://doi.org/10.1111/gcb.13679

Carroll, C., Parks, S. A., Dobrowski, S. Z., & Roberts, D. R. (2018). Climatic, topographic, and anthropogenic factors determine connectivity between current and future climate analogs in North America. *Global Change Biology,* gcb.14373. https://doi.org/10.1111/gcb.14373

Carroll, C., & Ray, J. C. (2021). Maximizing the effectiveness of national commitments to protected area expansion for conserving biodiversity and ecosystem carbon under climate change. *Global Change Biology,* gcb.15645. https://doi.org/10.1111/gcb.15645

Cushman, S. A., McKelvey, K. S., & Schwartz, M. K. (2009). Use of Empirically Derived Source-Destination Models to Map Regional Conservation Corridors. *Conservation Biology, 23(2),* 368–376. https://doi.org/10.1111/j.1523-1739.2008.01111.x

Dickson, B. G., Roemer, G. W., McRae, B. H., & Rundall, J. M. (2013). Models of Regional Habitat Quality and Connectivity for Pumas (Puma concolor) in the Southwestern United States. *PLoS ONE, 8(12),* e81898. https://doi.org/10.1371/journal.pone.0081898

Dinerstein, E., Vynne, C., Sala, E., Joshi, A. R., Fernando, S., Lovejoy, T. E., Mayorga, J., Olson, D., Asner, G. P., Baillie, J. E. M., Burgess, N. D., Burkart, K., Noss, R. F., Zhang, Y. P., Baccini, A., Birch, T., Hahn, N., Joppa, L. N., & Wikramanayake, E. (2019). A Global Deal For Nature: Guiding principles, milestones, and targets. *Science Advances, 5(4),* eaaw2869. https://doi.org/10.1126/sciadv.aaw2869

Dinerstein, Eric, Olson, D., Joshi, A., Vynne, C., Burgess, N. D., Wikramanayake, E., Hahn, N., Palminteri, S., Hedao, P., Noss, R., Hansen, M., Locke, H., Ellis, E. C., Jones, B., Barber, C. V., Hayes, R., Kormos, C., Martin, V., Crist, E., … Saleem, M. (2017). An Ecoregion-Based Approach to Protecting Half the Terrestrial Realm. *BioScience, 67(6),* 534–545. https://doi.org/10.1093/biosci/bix014

Doyle, Martin W. & F. Douglas Shields. (2012). Compensatory Mitigation for Streams Under the Clean Water Act: Reassessing Science and Redirecting Policy. *Journal of the American Water Resources Association (JAWRA) 48(3),* 494-509.

Elsen, P. R., Monahan, W. B., Dougherty, E. R., & Merenlender, A. M. (2020). Keeping pace with climate change in global terrestrial protected areas. *Science Advances, 6(25),* eaay0814. https://doi.org/10.1126/sciadv.aay0814

Environmental Protection Agency (EPA). (2006). Ecoregions of North America. https://www.epa.gov/eco-research/ecoregions-north-america

Favata, C. A., A. Maia, M. Pant, V. Nepal, & R. E. Colombo. (2018). Fish assemblage change following the structural restoration of a degraded stream. *River Research and Applications 34(8),* 927-936.

Fei, S., J. M. Desprez, K. M. Potter, I. Jo, J. A. Knott & C. M. Oswalt. Divergence of species responses to climate change. (2017). *Science Advances 3(5),* e1603055. https://doi.org/10.1126/sciadv.1603055

Franks, S. J., & Hoffmann, A. A. (2012). Genetics of Climate Change Adaptation. *Annual Review of Genetics, 46(1),* 185–208. https://doi.org/10.1146/annurev-genet-110711-155511

Garibaldi, L. A., Oddi, F. J., Miguez, F. E., Bartomeus, I., Orr, M. C., Jobbágy, E. G., Kremen, C., Schulte, L. A., Hughes, A. C., Bagnato, C., Abramson, G., Bridgewater, P., Carella, D. G., Díaz, S., Dicks, L. V., Ellis, E. C., Goldenberg, M., Huaylla, C. A., Kuperman, M., … Zhu, C. (2021). Working landscapes need at least 20% native habitat. Conservation Letters, 14(2). https://doi.org/10.1111/conl.12773

Gray, C. L., Hill, S. L. L., Newbold, T., Hudson, L. N., Börger, L., Contu, S., Hoskins, A. J., Ferrier, S., Purvis, A., & Scharlemann, J. P. W. (2016). Local biodiversity is higher inside than outside terrestrial protected areas worldwide. *Nature Communications, 7(1),* 12306. https://doi.org/10.1038/ncomms12306

Groves, C. R., Game, E. T., Anderson, M. G., Cross, M., Enquist, C., Ferdaña, Z., Girvetz, E., Gondor, A., Hall, K. R., Higgins, J., Marshall, R., Popper, K., Schill, S., & Shafer, S. L. (2012). Incorporating climate change into systematic conservation planning. *Biodiversity and Conservation*, *21*(7), 1651–1671. https://doi.org/10.1007/s10531-012-0269-3

Hamann, A., Roberts, D. R., Barber, Q. E., Carroll, C., & Nielsen, S. E. (2015). Velocity of climate change algorithms for guiding conservation and management. *Global Change Biology*, *21*(2), 997–1004. https://doi.org/10.1111/gcb.12736

Hausfather, Z., & Peters, G. P. (2020). RCP8.5 is a problematic scenario for near-term emissions. *Proceedings of the National Academy of Sciences, 117(45),* 27791–27792. https://doi.org/10.1073/pnas.2017124117

International Energy Agency (IEA). (2019). World Energy Outlook 2019. https://www.iea.org/reports/world-energy-outlook-2019

Intergovernmental Pannel of Climate Change (IPCC). (2014). Climate Change 2014: Synthesis Report. Contribution of Working Groups I, II and III to the Fifth Assessment Report of the Intergovernmental Panel on Climate Change [Core Writing Team, R.K. Pachauri and L.A. Meyer (eds.)]. IPCC, Geneva, Switzerland. https://www.ipcc.ch/report/ar5/syr/

Isaak, D.J.; Wenger, S.J.; Peterson, E.E.; Ver Hoef, J.M.; Hostetler, S.W.; Luce, C.H.; Dunham, J.B.; Kershner, J.L.; Roper, B.B.; Nagel, D.E.; Chandler, G.L.; Wollrab, S.P.; Parkes, S.L.; Horan, D.L. (2016). NorWeST modeled summer stream temperature scenarios for the western U.S. Fort Collins, CO: Forest Service Research Data Archive. https://doi.org/10.2737/RDS-2016-0033.

Jantarasami, L.C., Novak, R., Delgado, R., Marino, E., McNeeley, S., Narducci, C., Raymond-Yakoubian, J., Singletary, L., and K. Powys Whyte. (2018). Tribes and Indigenous Peoples. In Impacts, Risks, and Adaptation in the United States: Fourth National Climate Assessment, Volume II [Reidmiller, D.R., Avery, C.W., Easterling, D.R., Kunkel, K.E., Lewis, K.L.M., Maycock, T.K., & Stewart, B.C. (eds.)]. U.S. Global Change Research Program, Washington, DC, USA, pp. 572–603. doi: 10.7930/NCA4.2018.CH15

Jayakarana, A.D., Z.T. Smoot, D.M. Park, and D.R. Hitchcock. (2016). Relating stream function and land cover in the Middle Pee Dee River Basin, SC. *Journal of Hydrology Regional Studies, 5,* 261–275.

Jenkins, C. N., Van Houtan, K. S., Pimm, S. L., & Sexton, J. O. (2015). US protected lands mismatch biodiversity priorities. *Proceedings of the National Academy of Sciences, 112(16),* 5081–5086. https://doi.org/10.1073/pnas.1418034112

Keppel, G., & Wardell-Johnson, G. W. (2012). Refugia: Keys to climate change management. *Global Change Biology, 18(8),* 2389–2391. https://doi.org/10.1111/j.1365-2486.2012.02729.x

Kraus, D., & Hebb, A. (2020). Southern Canada's crisis ecoregions: Identifying the most significant and threatened places for biodiversity conservation. *Biodiversity and Conservation, 29(13),* 3573–3590. https://doi.org/10.1007/s10531-020-02038-x

Lee-Ashley, M., Rowland-Shea, J. & Richards, R. (2019). The Green Squeeze. Washington, D.C., Center for American Progress. https://www.americanprogress.org/issues/green/reports/2019/10/22/476220/the-green-squeeze/

Letcher, B., et al. (2017). Brook Trout Probability of Occurrence. Northeast U.S. North Atlantic Landscape Conservation Cooperative.

Lewis, K. E., Rota, C. T., Lituma, C. M., & Anderson, J. T. (2019). Influence of the Agricultural Conservation Easement Program wetland practices on winter occupancy of Passerellidae sparrows and avian species richness. PLOS ONE, 14(1), e0210878. https://doi.org/10.1371/journal.pone.0210878

Littlefield, C. E., McRae, B. H., Michalak, J. L., Lawler, J. J., & Carroll, C. (2017). Connecting today's climates to future climate analogs to facilitate movement of species under climate change: Climate Change and Species' Movement. *Conservation Biology*, *31*(6), 1397–1408. https://doi.org/10.1111/cobi.12938

Locke, H. (2013). Nature needs half: A necessary and hopeful new agenda for protected areas. *PARKS, 19(2),* 13–22. https://doi.org/10.2305/IUCN.CH.2013.PARKS-19-2.HL.en

620 Lookingbill, T. R., Gardner, R. H., Ferrari, J. R., & Keller, C. E. (2010). Combining a dispersal
621 model with network theory to assess habitat connectivity. *Ecological Applications, 20(2),*
622 427–441. https://doi.org/10.1890/09-0073.1
623
624 Maxwell, S. L., Cazalis, V., Dudley, N., Hoffmann, M., Rodrigues, A. S. L., Stolton, S.,
625 Visconti, P., Woodley, S., Kingston, N., Lewis, E., Maron, M., Strassburg, B. B. N.,
626 Wenger, A., Jonas, H. D., Venter, O., & Watson, J. E. M. (2020). Area-based
627 conservation in the twenty-first century. *Nature*, *586*(7828), 217–227.
628 https://doi.org/10.1038/s41586-020-2773-z
629
630 McClure, M. L., Hansen, A. J., & Inman, R. M. (2016). Connecting models to movements:
631 Testing connectivity model predictions against empirical migration and dispersal data.
632 *Landscape Ecology, 31(7),* 1419–1432. https://doi.org/10.1007/s10980-016-0347-0
633
634 McGuire, J. L., Lawler, J. J., McRae, B. H., Nuñez, T. A., & Theobald, D. M. (2016). Achieving
635 climate connectivity in a fragmented landscape. *Proceedings of the National Academy of*
636 *Sciences*, *113*(26), 7195–7200. https://doi.org/10.1073/pnas.1602817113
637
638 Melillo, J. M., Lu, X., Kicklighter, D. W., Reilly, J. M., Cai, Y., & Sokolov, A. P. (2016).
639 Protected areas' role in climate-change mitigation. *Ambio, 45(2),* 133–145.
640 https://doi.org/10.1007/s13280-015-0693-1
641
642 Merriam, E. R., J. T. Petty, & J. Clingerman. (2019). Conservation planning at the intersection of
643 landscape and climate change: brook trout in the Chesapeake Bay watershed. *Ecosphere,*
644 *10(2),* e02585.
645
646 Michalak, J. L., Lawler, J. J., Roberts, D. R., & Carroll, C. (2018). Distribution and protection of
647 climatic refugia in North America: Climatic Refugia. *Conservation Biology*, *32*(6), 1414–
648 1425. https://doi.org/10.1111/cobi.13130

649 Michalak, J. L., D. Stralberg, J. M. Cartwright, & J. J. Lawler. (2020). Combining physical and
650 species-based approaches improves refugia identification, *Front Ecol Environ 18(5),* 254–
651 260.

652 Monzón, J., Moyer-Horner, L., & Palamar, M. B. (2011). Climate Change and Species Range
653 Dynamics in Protected Areas. *BioScience, 61(10),* 752–761.
654 https://doi.org/10.1525/bio.2011.61.10.5
655

656 Morelli, T. L., C. Daly, S. Z. Dobrowski, D.M. Dulen, J. L. Ebersole, & S. T. Jackson, et al. (2016).
657 Managing climate change refugia for climate adaptation. *PLoS ONE, 11(8),* e0159909.

658 Morelli, T. L., C. W Barrows, A. R. Ramirez, J. M. Cartwright, D. D. Ackerly, T. D. Eaves, J. L.
659 Ebersole, et al. (2020). Climate-change refugia: biodiversity in the slow lane. *Front Ecol*
660 *Environ, 18(5),* 228–234.

661 Myers, N., Mittermeier, R. A., Mittermeier, C. G., da Fonseca, G. A. B., & Kent, J. (2000).
662 Biodiversity hotspots for conservation priorities. *Nature, 403(6772),* 853–858.
663 https://doi.org/10.1038/35002501
664

665 National Fish, Wildlife, and Plants Climate Adaptation Network (NFWPCAN). (2021).
666 Advancing the national fish, wildlife, and plants climate adaptation strategy into a new
667 decade. Association of Fish and Wildlife Agencies, Washington, DC.
668 https://www.fishwildlife.org/application/files/4216/1161/3356/Advancing_Strategy_Rep
669 ort_FINAL.pdf
670

671 National Academy of Sciences, Engineering, and Medicine (NASEM). (2016). A review of the
672 Landscape Conservation Cooperative. Washington, DC: The National Academies Press.
673 https://doi.org/10.17226/21829
674

675 Nature Conservancy, The. (2020). Resilient Land Mapping tool.
676 https://maps.tnc.org/resilientland/
677

678 Neilson, R. P., Pitelka, L. F., Solomon, A. M., Nathan, R., Midgley, G. F., Fragoso, J. M. V.,
679 Lischke, H., & Thompson, K. (2005). Forecasting Regional to Global Plant Migration in
680 Response to Climate Change. *BioScience, 55(9),* 749. https://doi.org/10.1641/0006-
681 3568(2005)055[0749:FRTGPM]2.0.CO;2
682
683 Newsom, G. (2020). Executive Order N-82-20. https://www.gov.ca.gov/wp-
684 content/uploads/2020/10/10.07.2020-EO-N-82-20-signed.pdf
685
686 Pörtner, H.O., Scholes, R.J., Agard, J., Archer, E., Arneth, A., Bai, X., Barnes, D., Burrows, M.,
687 Chan, L., Cheung, W.L., Diamond, S., Donatti, C., Duarte, C., Eisenhauer, N., Foden,
688 W., Gasalla, M. A., Handa, C., Hickler, T., Hoegh-Guldberg, O., Ichii, K., Jacob, U.,
689 Insarov, G., Kiessling, W., Leadley, P., Leemans, R., Levin, L., Lim, M., Maharaj, S.,
690 Managi, S., Marquet, P. A., McElwee, P., Midgley, G., Oberdorff, T., Obura, D.,
691 Osman, E., Pandit, R., Pascual, U., Pires, A. P. F., Popp, A., ReyesGarcía, V.,
692 Sankaran, M., Settele, J., Shin, Y. J., Sintayehu, D. W., Smith, P., Steiner, N.,
693 Strassburg, B., Sukumar, R., Trisos, C., Val, A.L., Wu, J., Aldrian, E., Parmesan, C.,
694 Pichs-Madruga, R., Roberts, D.C., Rogers, A.D., Díaz, S., Fischer, M., Hashimoto, S.,
695 Lavorel, S., Wu, N., Ngo, H.T. (2021). IPBES-IPCC co-sponsored workshop report on
696 biodiversity and climate change; IPBES and IPCC. DOI:10.5281/zenodo.4782538
697
698 Rights and Resources Initiative. (2020). Rights-Based Conservation: The path to preserving
699 Earth's biological and cultural diversity? Washington, DC: Rights and Resources
700 Initiative.
701
702 Román-Palacios, C., & Wiens, J. J. (2020). Recent responses to climate change reveal the drivers
703 of species extinction and survival. *Proceedings of the National Academy of Sciences,*
704 *117(8),* 4211–4217. https://doi.org/10.1073/pnas.1913007117
705
706 Rosa, L. & J. Malcom. (2020). Getting to 30x30: Guidelines for decision makers. Defenders of
707 Wildlife. https://defenders.org/sites/default/files/2020-07/getting-to-30x30-guidelines-
708 for-decision-makers.pdf

Saxon, E. (2008). Noah's Parks: A partial antidote to the Anthropocene extinction event. *Biodiversity*, *9*(3–4), 5–10. https://doi.org/10.1080/14888386.2008.9712901

Scott, J. M., Davis, F. W., McGhie, R. G., Wright, R. G., Groves, C., & Estes, J. (2001). Nature reserves: Do they capture the full range of America's biological diversity? *Ecological Applications, 11(4)*, 999–1007. https://doi.org/10.1890/1051-0761(2001)011[0999:NRDTCT]2.0.CO;2

Soto-Navarro, C., Ravilious, C., Arnell, A., de Lamo, X., Harfoot, M., Hill, S. L. L., Wearn, O. R., Santoro, M., Bouvet, A., Mermoz, S., Le Toan, T., Xia, J., Liu, S., Yuan, W., Spawn, S. A., Gibbs, H. K., Ferrier, S., Harwood, T., Alkemade, R., … Kapos, V. (2020). Mapping co-benefits for carbon storage and biodiversity to inform conservation policy and action. Philosophical Transactions of the Royal Society B: Biological Sciences, 375(1794), 20190128. https://doi.org/10.1098/rstb.2019.0128

Simmons, B. A., Nolte, C., & McGowan, J. (2021). Delivering on Biden's 2030 conservation commitment [Preprint]. *Ecology*. https://doi.org/10.1101/2021.02.28.433244

Stolton, S., Dudley, N., Çokçalışkan, B. A., Hunter, D., Ivanić, N., Kanga, E., Kettunen, M., Kumagai, Y., Maxted, N., Senior, J., Wong, M., Keenleyside, K., Mulrooney, D., & Withaka, J. (2015). Values and benefits of protected areas. In *Protected Area Governance and Management*. ANU Press.

Stralberg, D., Carroll, C., Pedlar, J. H., Wilsey, C. B., McKenney, D. W., & Nielsen, S. E. (2018). Macrorefugia for North American trees and songbirds: Climatic limiting factors and multi-scale topographic influences. *Global Ecology and Biogeography*, *27*(6), 690–703. https://doi.org/10.1111/geb.12731

738 Stralberg, D., D. Arseneault, J. L. Baltzer, Q. E. Barber, E. M. Bayne, Y. Boulanger, et al.
739 (2020a). Climate-change refugia in boreal North America: what, where, and for how
740 long? *Front Ecol Environ 18(5),* 261–270.
741
742 Stralberg, D., C. Carroll, & S. E. Nielsen. (2020b). Toward a climate-informed North American
743 protected areas network: Incorporating climate-change refugia and corridors in
744 conservation planning. *Conservation Letters,* e12712.
745
746 Stranko, S. A., R. H. Hilderbrand, R. P. Morgan II, M. W. Staley, A. J. Becker, A. Roseberry-
747 Lincoln, E. S. Perry, & P. T. Jacobson. (2008). Brook Trout Declines with Land Cover
748 and Temperature Changes in Maryland. *North American Journal of Fisheries*
749 *Management, 28,* 1223-1232.
750
751 Sullivan, S. M. P. & M. C. Watzin. (2009). Stream–floodplain connectivity and fish assemblage
752 diversity in the Champlain Valley, Vermont. *Journal of Fish Biology, 74,* 1394–1418.
753
754 Sweeney, B. W. & J. D. Newbold. (2014). Streamside Forest Buffer Width Needed to Protect
755 Stream Water Quality, Habitat, and Organisms: A Literature Review. *Journal of the*
756 *American Water Resources Association (JAWRA), 50(3),* 560-584.
757
758 Theoharides, K. (2014). Seeds of Resilience: Safeguarding Wildlife and Habitat from Climate
759 Change through the Farm Bill Conservation Programs. Defenders of Wildlife.
760 https://defenders.org/sites/default/files/publications/seeds-of-resilience-safeguarding-
761 wildlife-and-habitat-from-climate-change-through-the-farm-bill-conservation-
762 programs.pdf
763
764 United Nations Environment Program Convention on Biological Diversity (2020). Zero draft of
765 the post-2020 global biodiversity framework.
766 https://www.cbd.int/doc/c/efb0/1f84/a892b98d2982a829962b6371/wg2020-02-03-en.pdf
767

U.S. Fish and Wildlife Service (USFWS) & Association of Fish and Wildlife Agencies (AFWA). (2017). Guidance for Wildlife Action Plan Review and Revision. https://fawiki.fws.gov/download/attachments/5931146/2017%20Guidance%20on%20Wildlife%20Action%20Plan%20Review%20and%20Revision.pdf?version=1&modificationDate=1512664258000&api=v2

U.S. Geological Survey (USGS) Gap Analysis Project (GAP). (2020). Protected Areas Database of the United States (PAD-US) 2.1. U.S. Geological Survey data release, https://doi.org/10.5066/P92QM3NT.

U.S. Departments of Interior (DOI), Agriculture, Commerce, and the Council on Environmental Quality. (2021). Conserving and Restoring American the Beautiful. https://www.doi.gov/sites/doi.gov/files/report-conserving-and-restoring-america-the-beautiful-2021.pdf

Venter, O., Magrach, A., Outram, N., Klein, C. J., Possingham, H. P., Di Marco, M., & Watson, J. E. M. (2018). Bias in protected-area location and its effects on long-term aspiration of biodiversity conventions. Conservation Biology, 32(1), 127-134. https://doi.org/10.1111/cobi.12970

Vose, R. S., Easterling, D. R., Kunkel, K. E., LeGrande, A. N., & Wehner, M. F. (2017). Ch. 6: Temperature Changes in the United States. Climate Science Special Report: Fourth National Climate Assessment, Volume I. U.S. Global Change Research Program. https://doi.org/10.7930/J0N29V45

Wiens, J. J. (2016). Climate-Related Local Extinctions Are Already Widespread among Plant and Animal Species. *PLOS Biology, 14(12),* e2001104. https://doi.org/10.1371/journal.pbio.2001104

Wuebbles, D. J., Fahey, D. W., Hibbard, K. A., Dokken, D. J., Stewart, B. C., & Maycock, T. K. (2017). Climate Science Special Report: Fourth National Climate Assessment, Volume I. U.S. Global Change Research Program. https://doi.org/10.7930/J0J964J6

TABLES AND FIGURES

Table 1. Description of refugia datasets. Classes are based on results from a principal components analysis where component 1 (topodiversity) explained 33.8%, component 2 (climate stability) explained 15.9% and component 3 (tree macrorefugia) explained near 13.8% of variation. See SI for additional details.

Refugia Class	Dataset	Description	Source
Topodiversity	Current Climate Diversity	*Climate-Based.* Based on 11 bioclimatic variables using climate data for a 30-year climate normal period (1981-2010).	Carroll et al., 2017
	Ecotypic Diversity	*Landscape-based and climate-based.* Derived from edaphic, climatic, and landcover data.	Carroll et al., 2017
	Land Facet Diversity	*Landscape-based.* Incorporated elevation, latitude-adjusted elevation, topographic position index, slope, modified heat load index, and soil.	Carroll et al., 2017
	Landscape Diversity	*Landscape-based.* Described the diversity of microhabitats and climatic gradients. Microclimates were measured by quantifying elevation range, the variety of small-scale landforms, and the density and configuration of wetlands in a 100-acre neighborhood.	The Nature Conservancy, 2020
	Bird Macrorefugia	*Climate-based and species-based.* Focused on regions where the current and projected future species ranges overlap. Input based on current species niches for 268 songbird species; climate velocity based on 4 representative GCMs, RCP 4.5, 2080s.	Stralberg et al., 2018
Climatic Stability	Climatic Dissimilarity	*Climate-based.* Described how different the future climate at a location will be from its current climate. Measured in terms of multivariate climate characteristics, via a principal components analysis (PCA) of 11 biologically-relevant temperature and precipitation variables, RCP 4.5, 2080s.	Belote et al., 2018
	Climate Velocity	*Climate-based.* Velocity was calculated by dividing the rate of climate change by the rate of spatial climate variability to focus on regions where climatic conditions move more slowly across the landscape. Input based on A2 emissions scenarios implemented by seven GCMs of the CMIP3 multimodel dataset, RCP 4.5, 2080s.	AdaptWest Project, 2015
Tree Macrorefugia	Tree Macrorefugia	*Climate-based and species-based.* Focused on regions where the current and projected future species ranges overlapped. Input based on current species niches for 324 tree species; climate velocity based on 4 representative GCMs, RCP 4.5, 2080s.	Stralberg et al., 2018

826

827 **Table 2.** Overlays of national-level datasets representing protected areas, carbon stores,
828 biodiversity, climate refugia, and climate corridors. Values represent the percent of each top line
829 item (column) that falls within each row. Values in parentheses are the percent of total CONUS
830 area represented by the overlay.

% of top line items that fall into each of the following:	**GAP 1 & 2**	**GAP 3**	**Top 20% Carbon**	**Top 20% Biodiversity**	**Top 20% Refugia**	**Top 20% Climate-Informed Corridors**
GAP 1 & 2	100 (7.5)	0.0 (0.0)	12.7 (2.4)	3.7 (0.7)	13.3 (2.6)	13.8 (2.7)
GAP 3	0.0 (0.0)	100 (16.6)	20.2 (3.9)	5.1 (1.0)	25.0 (4.8)	30.4 (6.0)
Top 20% Carbon	32.8 (2.4)	23.3 (3.9)	100 (20.0)	28.8 (5.6)	32.5 (6.2)	27.2 (5.4)
Top 20% Biodiversity	12.3 (0.7)	8.7 (1.0)	32.0 (5.6)	100 (20.0)	30.8 (5.9)	11.2 (1.8)
Top 20% Refugia	34.2 (2.6)	29.0 (4.8)	32.8 (6.2)	36.8 (5.9)	100 (20.0)	28.7 (5.7)
Top 20% Climate-Informed Corridors	36.5 (2.7)	36.3 (6.0)	25.8 (5.4)	9.3 (1.8)	29.6 (5.7)	100 (20.0)

Table 3. Overlays of ecoregion-specific datasets representing protected areas, carbon stores, biodiversity, climate refugia, and climate corridors. Values represent the percent of each top line item (column) that falls within each row. Values in parentheses are the percent of total CONUS area represented by the overlay.

% of top line items that fall into each of the following:	**GAP 1 & 2**	**GAP 3**	**Top 20% Carbon**	**Top 20% Biodiversity**	**Top 20% Refugia**	**Top 20% Climate-Informed Corridors**
GAP 1 & 2	100 (7.5)	0.0 (0.0)	1.1 (2.2)	8.6 (1.5)	12.2 (2.4)	13.8 (2.7)
GAP 3	0.0 (0.0)	100 (16.6)	17.9 (3.5)	17.7 (3.1)	19.6 (3.8)	30.4 (6.0)
Top 20% Carbon	29.8 (2.2)	21.2 (3.5)	100 (20.0)	28.0 (4.9)	21.7 (4.2)	26.1 (5.2)
Top 20% Biodiversity	18.4 (1.5)	17.5 (3.1)	26.4 (4.9)	100 (20.0)	22.0 (4.2)	17.5 (3.3)
Top 20% Refugia	31.4 (2.4)	22.7 (3.8)	21.3 (4.2)	24.2 (4.2)	100 (20.0)	25.9 (5.1)
Top 20% Climate-Informed Corridors	36.5 (2.7)	36.3 (6.0)	26.3 (5.2)	18.8 (3.3)	26.7 (5.1)	100 (20.0)

FIGURE LEGENDS

Figure 1. A) National-scale and B) ecoregion-specific refugia (top 20% of all three refugia classes combined) with climate-informed corridors (ecoregions are outlined in black). The full raster datasets were used to identify refugia in national analyses. Ecoregion-specific analyses

868 employ a stratified approach, where refugia are identified for each ecoregion separately before
869 combining them together. Ecoregions are outlined in black in map B.
870
871 **Figure 2.** Coincidence between national-scale and ecoregion-specific refugia. The full raster
872 datasets were used to identify refugia in national analyses. Ecoregion-specific analyses employ a
873 stratified approach, where refugia are identified for each ecoregion separately before combining
874 them together. Ecoregions are outlined in black.
875
876 **Figure 3.** Overlap between national-scale (A,B) and ecoregion-scale (C,D) refugia and corridors
877 with carbon stocks (B,D) and biodiversity hotspots (A,C). The full raster datasets were used to
878 identify refugia in national analyses. Ecoregion-specific analyses employ a stratified approach,
879 where refugia are identified for each ecoregion separately before combining them together.
880 Ecoregions outlined in black in maps C and D.
881
882 **Figure 4.** Overlap between national-scale refugia (A), climate corridors (B), and either refugia
883 or corridors (C) with the protected areas database of the US (PADUS). GAP codes are specific to
884 the management intent to conserve biodiversity; GAP 1 and 2 areas are managed in ways
885 typically consistent with conservation and GAP 3 areas are governed under multiple-use
886 mandates that may include biodiversity priorities but may also include incompatible activities.
887

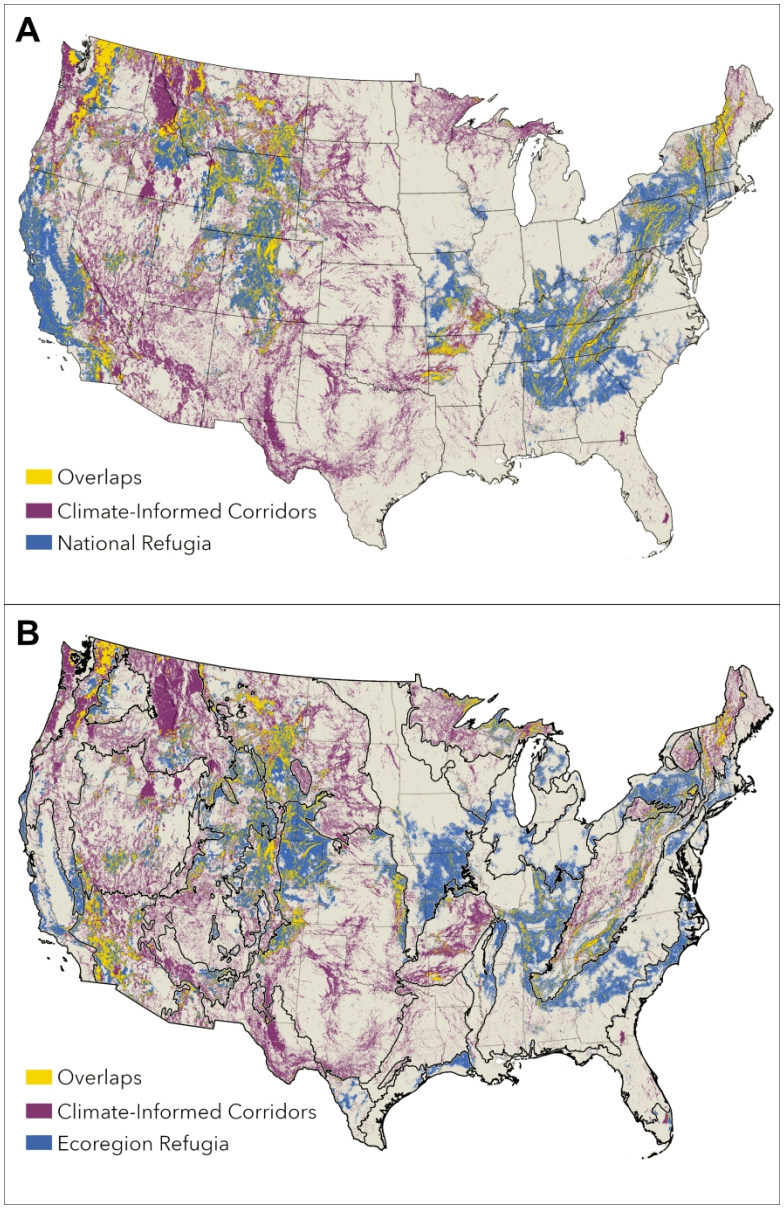

Figure 1. A) National-scale and B) ecoregion-specific refugia (top 20% of all three refugia classes combined) with climate-informed corridors (ecoregions are outlined in black). The full raster datasets were used to identify refugia in national analyses. Ecoregion-specific analyses employ a stratified approach, where refugia are identified for each ecoregion separately before combining them together. Ecoregions are outlined in black in map B.

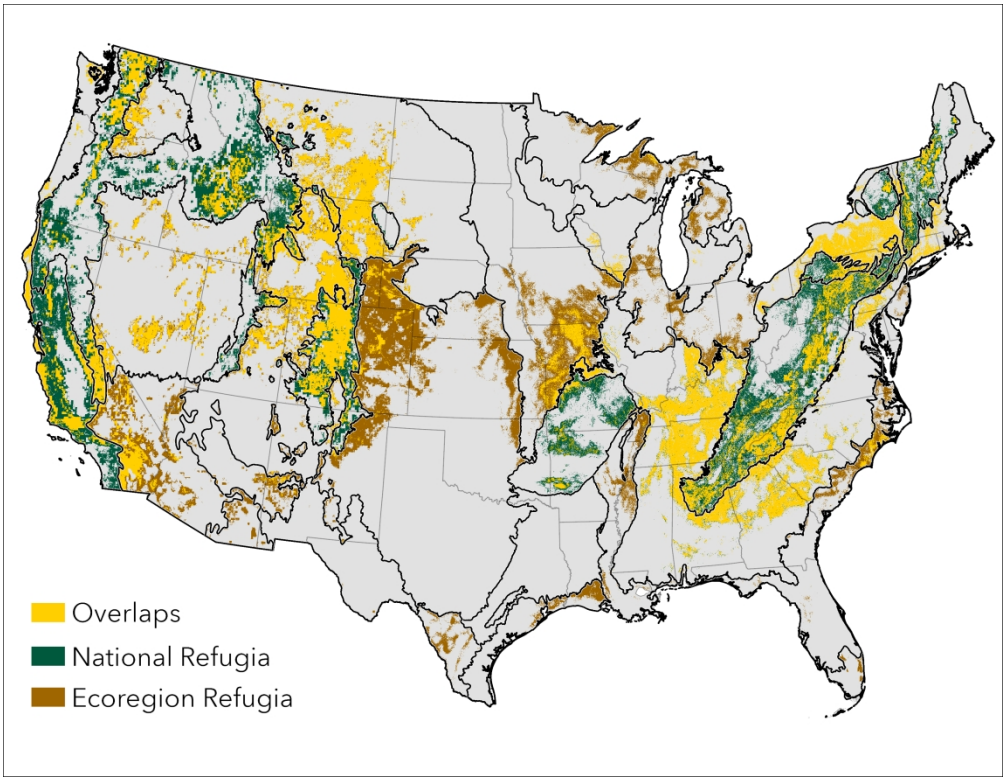

Figure 2. Coincidence between national-scale and ecoregion-specific refugia. The full raster datasets were used to identify refugia in national analyses. Ecoregion-specific analyses employ a stratified approach, where refugia are identified for each ecoregion separately before combining them together. Ecoregions are outlined in black.

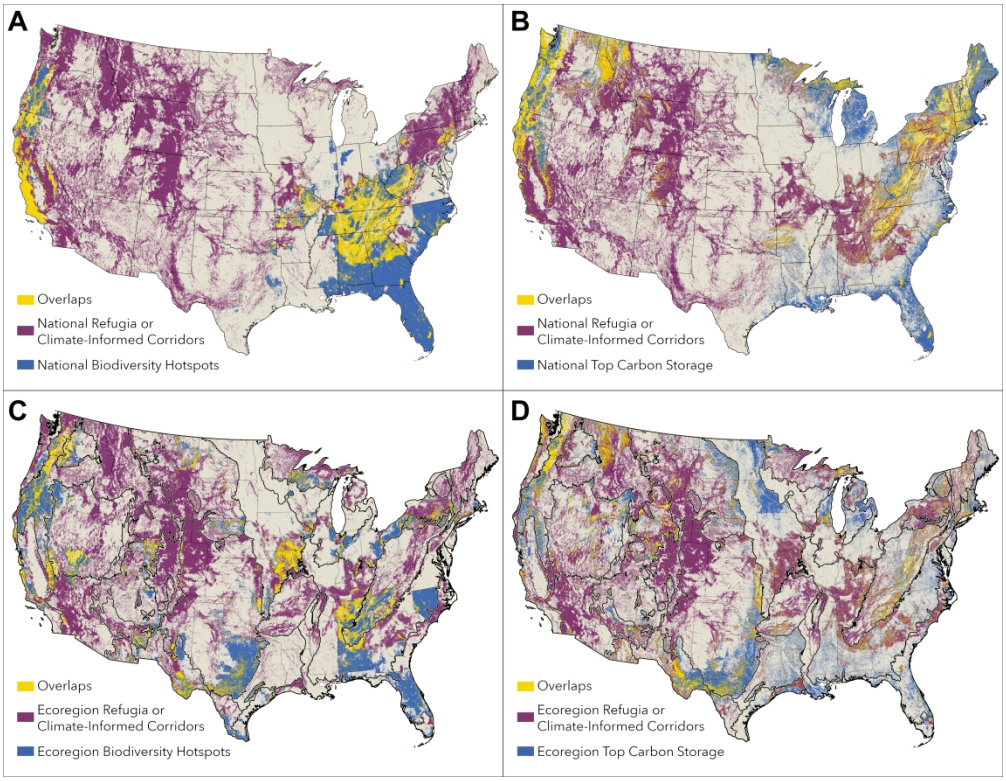

Figure 3. Overlap between national-scale (A,B) and ecoregion-scale (C,D) refugia and corridors with carbon stocks (B,D) and biodiversity hotspots (A,C). The full raster datasets were used to identify refugia in national analyses. Ecoregion-specific analyses employ a stratified approach, where refugia are identified for each ecoregion separately before combining them together. Ecoregions outlined in black in maps C and D.

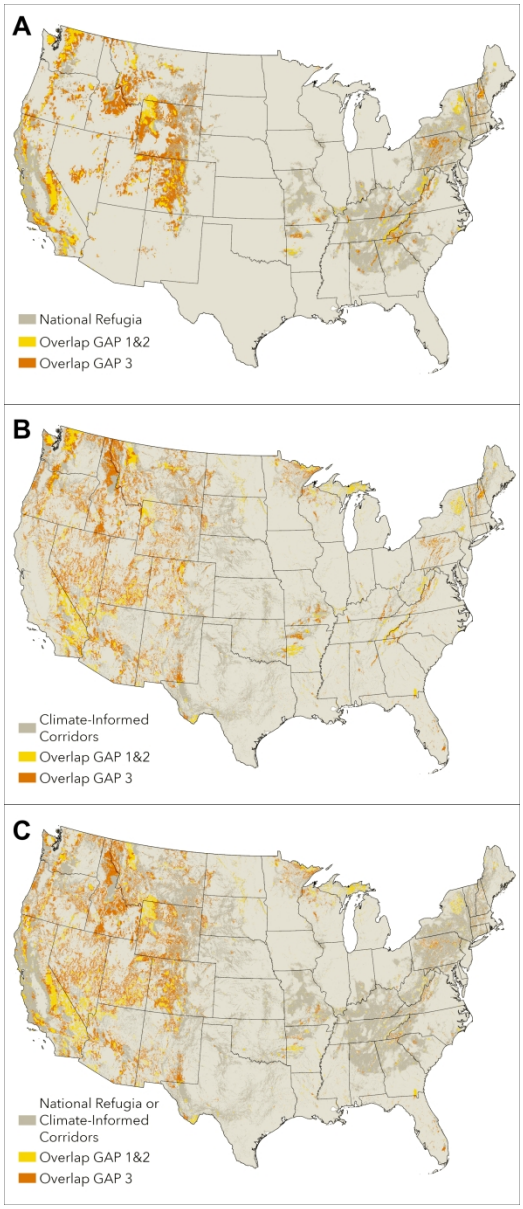

Figure 4. Overlap between national-scale refugia (A), climate corridors (B), and either refugia or corridors (C) with the protected areas database of the US (PADUS). GAP codes are specific to the management intent to conserve biodiversity; GAP 1 and 2 areas are managed in ways typically consistent with conservation and GAP 3 areas are governed under multiple-use mandates that may include biodiversity priorities but may also include incompatible activities.